Satellite-observed Snow Covered Area in the HBV-model

Final report

The DemoSnow project

Norwegian Space Centre contract JOP.8.3.3.11.01.3

Norwegian Water Resources and Energy Directorate
2002

Consultancy report Series A no 6

Satellite-observed Snow Covered Area in the HBV-model

Publisher: Norwegian Water Resources and Energy Directorate

Authors: Rune V. Engeset and Hans-Christian Udnæs

Print: NVE
Copies: 25
Pages: 32
Front page illustration: Snow covered area (SCA) observed by three different satellite sensors over Jotunheimen on 3 and 4 May 2000.
ISSN: 1503-0318

Summary: Spring snowmelt contributes significantly to floods with severe damages as the results, and updated snow information is very important to the Norwegian flood forecasting services, which uses the HBV-model to simulate runoff. Satellite imagery is used to observe the snow covered area (SCA), but these observations are not used directly in the hydrological simulations. This study assessed if runoff simulations could improve by application of satellite-derived snow data in the operational models, using both optical and radar satellite data. Three catchments in Jotunheimen, south Norway, were studied using eight years of data (1995-2002). The results show that satellite-observed SCA can be used to detect when the models do not simulate the snow reservoir correctly. Error detection early in the melt season helps the services to update and correct the models well in advance of damage floods. The method requires the models to be calibrated against SCA in addition to runoff. Data from the satellite sensors NOAA AVHRR and ERS SAR were used, of which AVHRR showed relatively good correlation with simulated SCA, but SAR at times showed high deviations. Comparison of simultaneous data from May 2000 from the sensors AVHRR, SAR, Terra MODIS and Landsat ETM+ showed good correlation. Of a total area of 1088 km^2, AVHRR observed a SCA of 823 km^2 and SAR 720 km^2, as compared to 889 km^2 using ETM+.

Key words: Snow, Satellite, Runoff

Norwegian Water Resources and Energy Directorate
Middelthuns gate 29
Box 5091 Majorstua
N-0301 OSLO

Telephone: +47 22 95 95 95
Fax: +47 22 95 90 00
Internet: www.nve.no

1 September 2002

Contents

Preface

The Norwegian Space Centre contributed half of the project costs and the project participants financed the rest (in total KNOK 564). The project was leaded by NVE, who participated together with the Norwegian Computing Centre and Norut IT. Liss M. Andreassen, and later Rune V. Engeset, NVE, lead the project. Project participants included Hans-Christian Udnæs and Eli Alfnes from NVE, Rune Solberg and Hans Koren from NR, and Tore Guneriussen and Erik Malnes from Norut IT.

This report documents the project work and results, and is complemented by project reports by NR on optical image processing and by Norut IT on radar image processing.

Oslo, 1 September 2002

Kjell Repp
Director

Erik Roland
Section manager

Summary

Snowmelt during the spring often contributes significantly to floods with severe damages as the results. An example is the large flood in south-east Norway in 1995. Thus, updated information on the snow conditions is very important to the national flood forecasting and preparedness services at NVE. At present, the HBV-model is used to simulate runoff in our river systems and satellite imagery are used to observe the snow covered area (SCA). However, the observed SCA is not used directly in the model simulations.

The objective of this project was to assess if runoff simulations could be improved by application of satellite-derived snow data in the operational models, using both optical and radar satellite data.

The HBV models used by the services were used to study three catchments in Jotunheimen, south Norway using eight years of data (1995-2002). The results show that satellite-observed SCA can be used for detecting when the hydrological models do not simulate the snow reservoir correctly. This is detected early in the melt season, helping the services to update and correct the models well in advance of damage floods later in the spring and summer. This makes the forecasting better and more precise, in particular during years when the snow reservoir deviates from the normal situation. A reason for having errors in the simulations is that observed precipitation and temperature do not represent the actual situation in the catchment. As a consequence, the models simulate a too large or too small snow volume or snow covered area, which is discovered when compared to the satellite observations. A prerequisite for detecting such deviations is that the models are calibrated against SCA in addition to runoff. SCA is presently the only model variable that may be observed relatively simply and efficiently over catchments with little forest.

The satellite sensors NOAA AVHRR and ERS SAR were used to derive time series of SCA. AVHRR-based data showed relatively good correlation with simulated SCA (deviation less than 10%). SAR-based data showed at times high deviation, which may be due to the problem of detecting dry snow. A comparison of simultaneous data (May 2002) from four satellites (NOAA AVHRR, Terra MODIS, ERS SAR and Landsat ETM+) gave a relatively good correlation. Of a total area of 1088 km^2 the SCA was observed as 823 km^2 using AVHRR and 720 km^2 using SAR, as compared to 889 km^2 using the ETM+ sensor, which was consider the reference.

Further work on improved satellite-based observation of snow extent, water equivalent, albedo and temperature is carried out together with development of new and better hydrological models. This work is carried out under the Norwegian Research Council project *SnowMan* (www.itek.norut.no/snowman) and the EU-projects *EnviSnow* (www.itek.norut.no/EnviSnow) and *EuroClim* (euroclim.nr.no).

1 Introduction

The Norwegian Water Resources and Energy Directorate (NVE), the Norwegian Computing Centre (NR) and Norut IT carried out the project (see Figure 1).

The objective of the project was to improve simulation of runoff using satellite-observed snow covered area (SCA) in an operational model. Five work packages were identified:

WP0 Administration
The project was managed by NVE.

WP1 Selection of study catchments
Three catchments were selected based on catchment characteristics, and the availability of hydrological, meteorological and satellite data. Mountain catchments are selected in order to reduce the uncertainty caused by vegetation. Four years of runoff and satellite data should be available at a weekly rate during the melt season.

WP2 Data processing
Historic satellite data covering the test catchments are transformed to a map projection and snow covered area (SCA) calculated for 1km * 1km or higher resolution. A total of approx. 12 optical and 12 radar images are processed for each catchment.

WP3 Model calibration
HBV models are calibrated for each test catchment using a period of minimum three years. The models are calibrated against both runoff and satellite-derived SCA. Models calibrated against runoff only are used for comparison in WP4.

WP4 Simulation and assessment
Model simulations are carried out for at least one independent year. Satellite-derived SCA is used for model SCA updating. Simulation of high-flow runoff is assessed in particular.

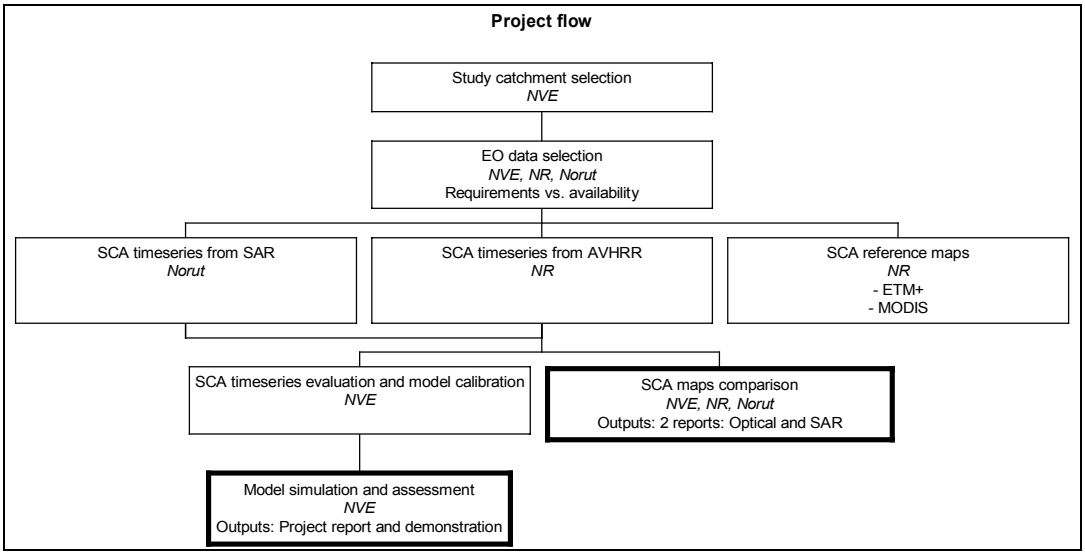

Figure 1 Project flow chart and deliverables.

2 Study area and data

2.1 Study catchments and hydrological data

The three test catchments Akslen, Sjodalsvatn and Vinde-elv were selected for the study, all located in the mountains in southern Norway (Figure 2). Meteorological stations were used for each catchment providing daily values of air temperature and precipitation. At the outlet defining each catchment, a runoff gauge provided daily discharge values. The catchment and data characteristics are listed in Table 1.

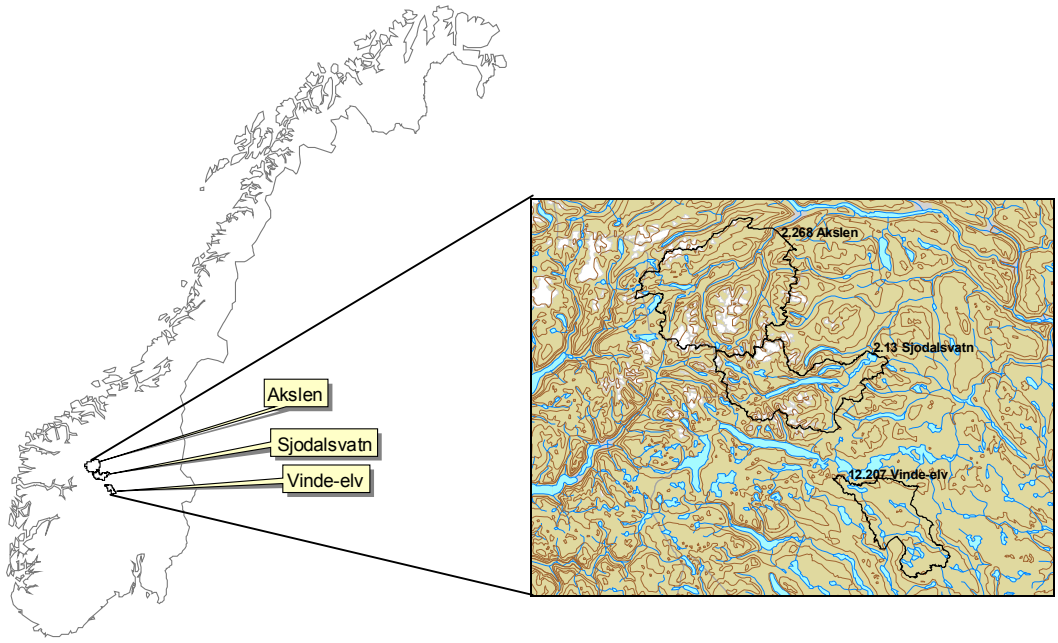

Figure 2 Location map of test catchments.

Table 1 Catchment characteristics and meteorological stations.

2.268 Akslen		**2.13 Sjodalsvatn**		**12.207 Vinde-elv**	
SCA range (%)	10-75	SCA range (%)	5-75	SCA range (%)	0-75
Area (km2)	791	Area (km2)	474	Area (km2)	268
Min elev. (m)	480	Min elev. (m)	940	Min elev. (m)	560
Med elev. (m)	1476	Med elev. (m)	1461	Med elev. (m)	985
Max elev. (m)	2472	Max elev. (m)	2400	Max elev. (m)	1680
Forest area (%)	13	Forest area (%)	5	Forest area (%)	31
Glacier area (%)	12	Glacier area (%)	9	Glacier area (%)	0
Lake area (%)	2	Lake area (%)	9	Lake area (%)	7
Mean flood (m3/s)	183	Mean flood (m3/s)	149	Mean flood (m3/s)	54
5-y flood (m3/s)	228	5-y flood (m3/s)	193	5-y flood (m3/s)	70
50-y flood (m3/s)	346	50-y flood (m3/s)	309	50-y flood (m3/s)	113
Meteorological stations:		*Meteorological stations:*		*Meteorological station:*	
T: 15430 Bøverdal	701 m a.s.l.	T: 13670 Skåbu-Storslåen	890 m a.s.l.	23420 Fagernes	365 m a.s.l.
P: 15730/20 Bråta	664 m a.s.l.	P: 13670 Skåbu-Storslåen	890 m a.s.l.		
		P: 15430 Bøverdal	701 m a.s.l.		

Akslen

Test site 1 Akslen (791 km^2) drains to the river Bøvra (Figure 3), where discharge (Figure 4) has been observed at gauge 2.268 Akslen since 1934. The catchment ranges from 480 to 2472 m a.s.l. (median of 1476). About 13 percent of the catchment are located below the tree line (958 m a.s.l. is used as the limit in the model), and glaciers cover 12 percent.

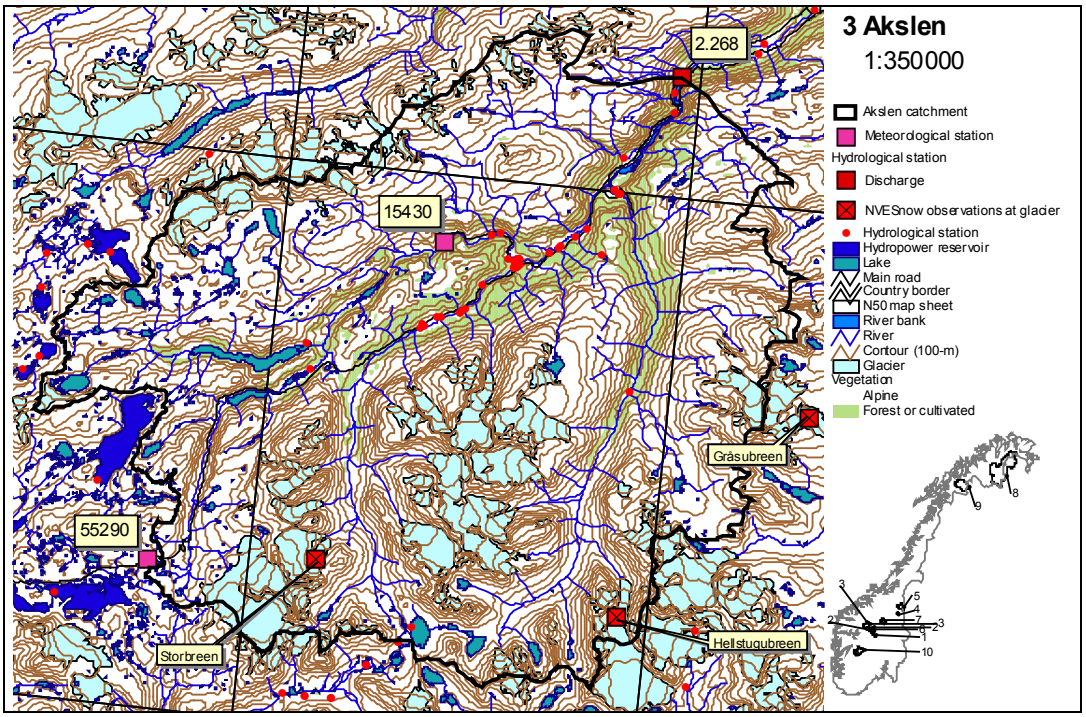

Figure 3 Akslen. The meteorological station Bråtå-Slettom (no. 15730) is situated 30 km north-west of Akslen. Data from Bråtå (no. 15720) is used until July 1998. In order to harmonise with data from 15720, precipitation data from 15730 was scaled by 1.135, and temperature data was subtracted 0.3 degrees. Precipitation station 55290 was not used.

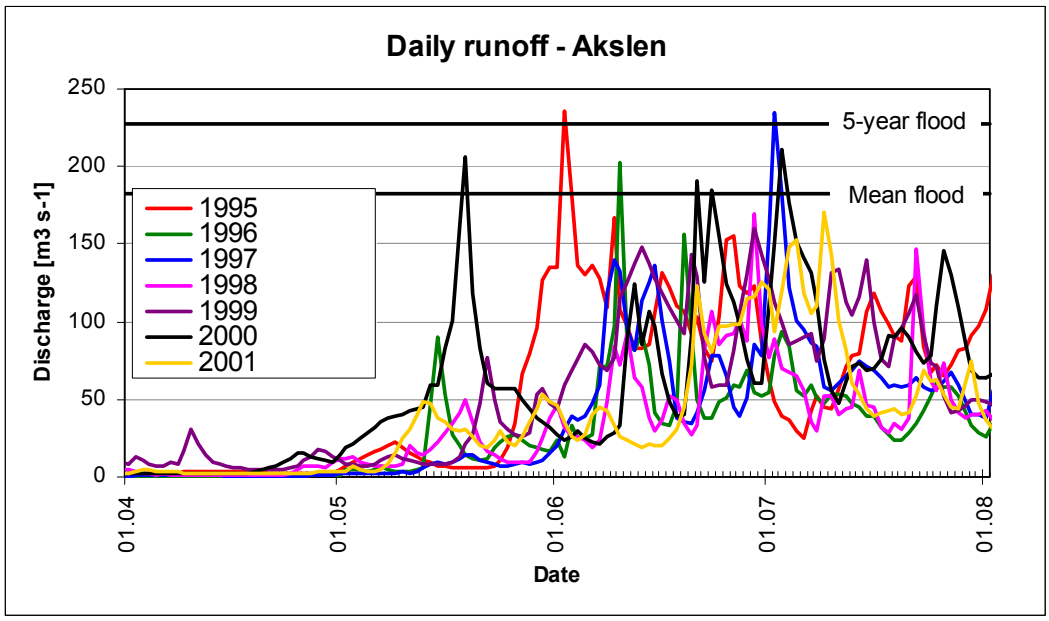

Figure 4 Discharge at Akslen.

Sjodalsvatn

Test site 2 drains to gauge 2.13 Sjodalsvatn in the river Sjoa (Figure 5), where discharge (Figure 6) has been observed since 1930. Its area covers 474 km^2 and ranges from 940 to 2400 m a.s.l. (median of 1461). Only about 5 percent of the catchment are below the tree line (1020 m a.s.l. is used as the limit in the model), and glaciers cover 9 percent.

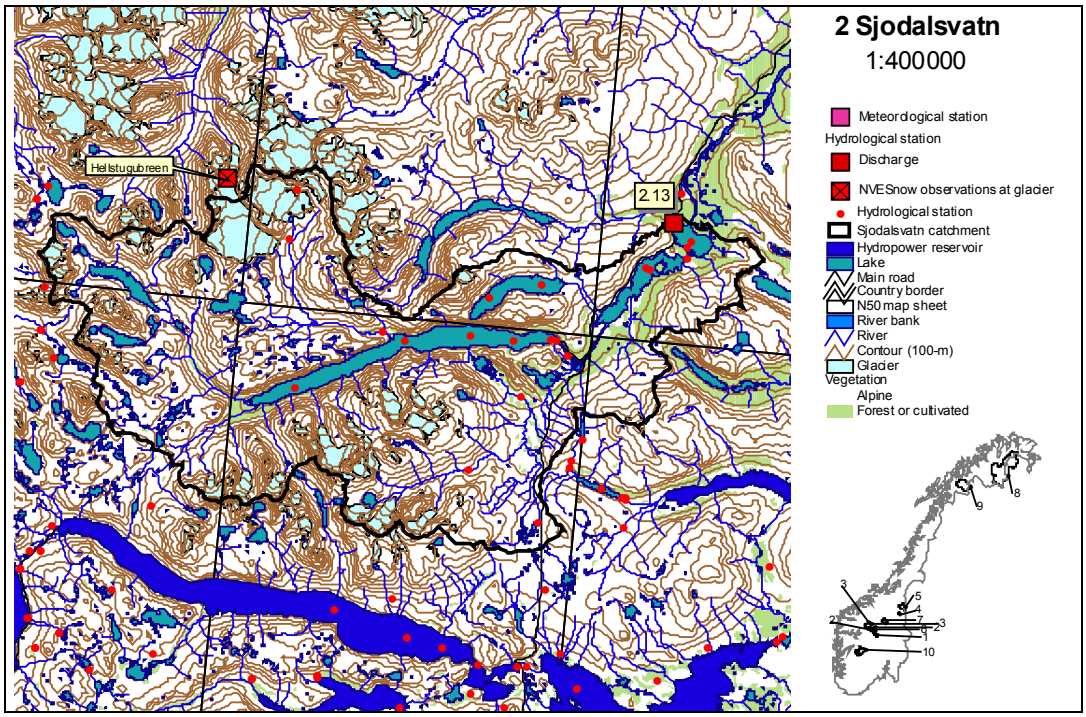

Figure 5 Sjodalsvatn. The meteorological stations Bøverdal (no. 15430) and Skåbu (no. 13670) are situated 30 km north-west and 20 km south-east of Sjodalsvatn. Precipitation was calculated as the average observed at Bøverdal and Skåbu.

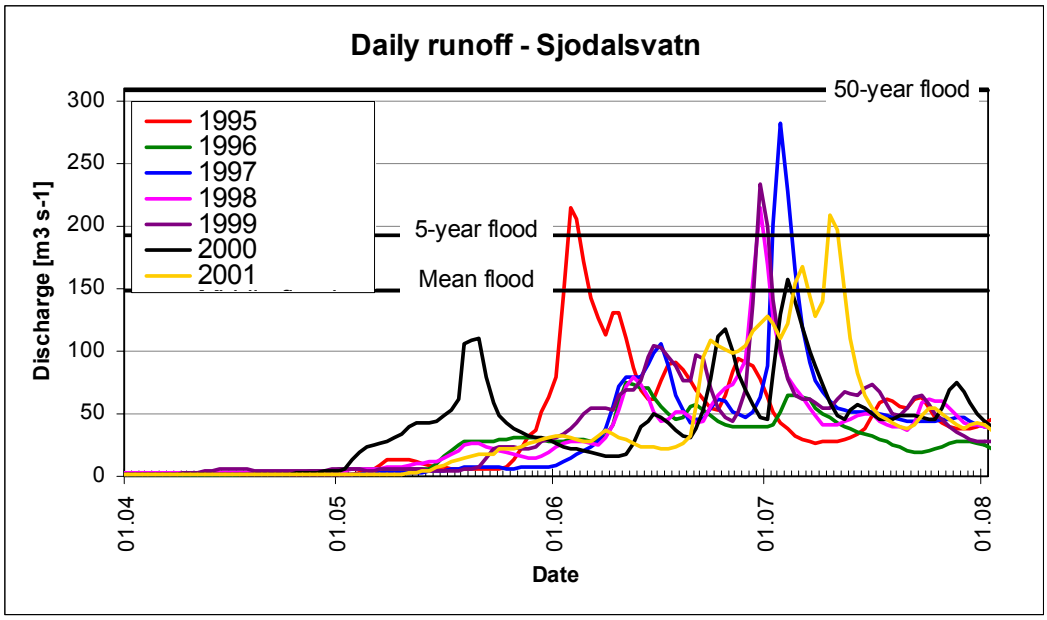

Figure 6 Discharge at Sjodalsvatn.

Vinde-elv

Test site 3 is the catchment that drains to the river Vinde (Figure 7). Discharge (Figure 8) has been observed at gauge 12.207 Vinde-elv from 1919. The 268 km^2 catchment ranges from 560 to 1686 m a.s.l. with a median elevation of 985. About 31 % of the area are located below the tree line (1015 m a.s.l. is used as the limit in the model), and there are no glaciers within the catchment.

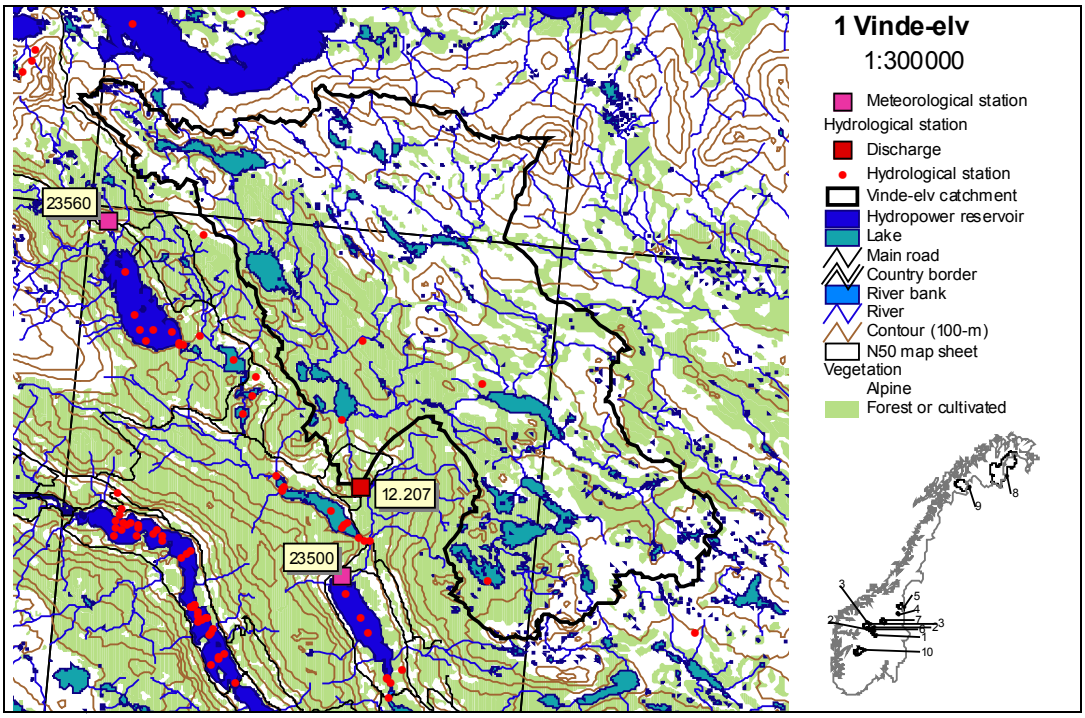

Figure 7 Vinde-elv. The meteorological station Fagernes (no. 23420) is situated 20 km south of Vinde-elv. Precipitation stations 23500 and 23560 were not used.

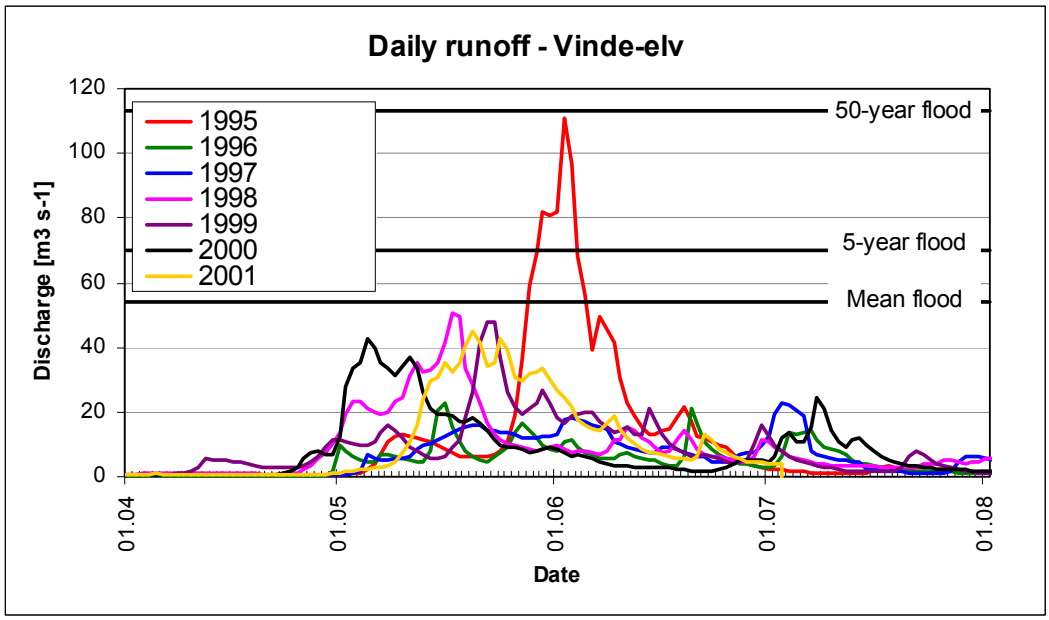

Figure 8 Discharge at Vinde-elv.

2.2 Satellite data

Data was compiled from the four satellite sensors NOAA AVHRR, Terra MODIS, Landsat ETM+ and ERS SAR. AVHRR and SAR data was used to produce the timeseries of SCA maps for use in the hydrological model. The ETM+ data was used as reference data for evaluating the SCA data retrieved from different sensors (AVHRR, MODIS, SAR). The MODIS data was used to make a simple assessment of the potential of MODIS as compared to AVHRR.

The following requirements were formulated for the SCA timeseries:

- SCA maps gives the percent snow covered area with 1 km by 1 km grid cells
- SCA maps are provided in the Arcinfo grid format in UTM projection and coordinate system zone 32, and WGS84 datum,
- One timeseries is require for each test catchment,
- Timeseries are composed from both optical and SAR data if possible,
- Timeseries composed from different EO-sensors or using different SCA retrieval algorithms are homogenised. The SCA maps should be within 10% of the true value, systematic differences removed, and the uncertainty quantified,
- The time series uses as many EO data acquisitions as possible for the melt period from 1 April to 31 July

The used data series covers the years 1995-2001 and is documented in Malnes and Guneriussen (2002) and Koren and Solberg (2002).

3 Methods

3.1 SCA-retrieval from satellite data

SCA was retrieved from EO data by NVE (pilot study), NR (optical data) and NORUT (SAR). NR's work is documented in Koren and Solberg (2002) and NORUT's in Malnes and Guneriussen (2002), see Annexes 3 and 4.

3.1.1 SCA-retrieval methods

3.1.1.1 NVE method for NOAA AVHRR data

The NVE method (Schjødt-Osmo and Engeset, 1997) derives SCA from AVHRR. Band 2 pixel values are converted into SCA using linear transformation, which is calibrated for each image using snow on glaciers for 100% SCA and snow-free land as 0 %.

3.1.1.2 NR method for NOAA AVHRR data

NR derives SCA from AVHRR using the band 2 based linear NLR algorithm (Solberg and Andersen 1994), and classifies SCA into six classes (Koren and Solberg 2002). Recent changes to the method produces percent SCA maps (from 1999).

3.1.1.3 NORUT method for ERS SAR data

NORUT converts SAR data into SCA using the Nagler algorithm (Nagler and Rott 2000, Malnes and Guneriussen 2002).

3.1.1.4 NR method for Landsat ETM+ data

SCA was estimated using an unsupervised clustering on bands 1-5 and 7 with 8 classes. The classes were reduced to three classes “No snow”, “Partly snow cover” and “Complete snow cover”.

3.1.1.5 NR method for Terra MODIS data

The SNOMAP algorithm (RIG 96) was applied to MODIS (bands 1, 2, 4 and 6) data, mapping snow cover at 500-m spatial resolution. A dummy land mask without water and a cloud mask without clouds were used to improve the snow cover map.

3.1.2 Comparison of SCA maps from different sensors

More detailed were carried out by NR and Norut IT, in which the SCA derived from the Landsat ETM+ image from 4 May 2001 was compared to AVHRR and MODIS (Koren and Solberg 2002), and ERS SAR (Malnes and Guneriussen 2002).

In this report the SCA derived from different sensors were compared on a catchment by catchment basis. Calculated SCA for the whole catchment, and for the part of the catchment located above the tree line were compared to simulated SCA and observed runoff, precipitation and temperatures. In this manner the effects of clouds, acquisition time-of-day etc could be assessed.

3.2 The HBV-model

The model used is based upon the Nordic HBV-model (a more detailed description is provided in Annex 2). The main structure of the HBV model is a sequence of submodels:

- snow submodel
- soil moisture zone
- dynamic part
- routing

The model is further structured in altitude intervals. This subdivision can be applied only to the snow submodel, or to the whole model. In the latter case, the height intervals can further be subdivided in one or two vegetation zones and lakes. Even when the model distributed on altitude intervals, the parameters are generally the same for all submodels. Interception, snow melt parameters and soil moisture capacity can however be varied according to vegetation type. The model can operate with up to 15 vegetation types, but usually not more than two or three would be activated.

3.3 SCA used in the HBV-model

3.3.1 SCA evaluation, selection and processing

The AVHRR and SAR based SCA timeseries were evaluated for use in the HBV-model calibration. Each SCA map was evaluated by the following criteria:

- The timeseries from NVE, NR and Norut should consistently describe the true change in SCA over time.
- Most of the catchment should be covered. If only parts of the catchment is covered, the maps should be discarded if the SCA map deviates from earlier or later acquisitions in a way that can not be corroborated using air temperature, precipitation or runoff data. Main problems expected were those induced by partial cloud cover (optical), low sun elevation (optical), dry snow (SAR), and other inter-sensor differences.

A combined timeseries of SCA maps was selected based on the evaluation and used for the model calibration. Simple correction algorithms were explored and applied where possible when systematic or physically based deviations were observed.

3.3.2 Model calibration

The HBV model was calibrated automatically for the three catchments using the parameter estimating routine PEST (Brebber et al., 1994). The model was calibrated in two modes for each catchment: first against runoff only, and secondly against both runoff and SCA. The optimal parameter sets from 96 PEST-calibrations from both modes were selected for further analysis.

3.3.3 Model simulations

The best parameter sets from the calibrations were used in simulations for the four validation years in order to evaluate the model consistency in time with respect to runoff and SCA.

3.3.4 Model updating

The working hypothesis was that the simulation of runoff and SCA could be improved in three ways:

1. ***Calibration***: Calibrating the model against runoff and SCA; or
2. ***Snow variable update***: Updated the model when a useful satellite observation of SCA was available, using rules for updating the SWE and SCA variables in the model. For example, the SWE could be updated by changing input precipitation or temperature, or adjusting the calibration variables such as the degree-day melt factor; or
3. ***Assembly update***: An assembly of calibrated models is compared with observations when a useful satellite observation of SCA was available. The model which best describe observed runoff and SCA is used for the next period until SCA is observed again.

4 Results and discussion

4.1 Pilot study

Due to delays in the delivery of EO-derived SCA data, NVE processed a number of AVHRR scenes into SCA maps in order to assess the use of EO-derived SCA in the HBV-model. This preliminary analysis is documented in Udnæs et al. (2002), see Annex 2, and summarised as follows:

1. SCA was derived from optical satellite imagery to test if the hydrological model may simulate runoff better if it is calibrated using SCA data in addition to runoff.
2. HBV models are calibrated for 3 catchments in the mountainous area in southern Norway. Several parameter sets are calibrated automatically against runoff, and against runoff and SCA for the three years 1997, 1998 and 1999.
3. Simulations are then carried out for the verification years 1995, 1996 and 2000.
4. For all catchments the additional calibration against SCA caused clear improvements in simulation of SCA. For two of the catchments there was minor reductions in the precision of the runoff simulations.
5. In the simulation period, the models calibrated against SCA and runoff did not prove to simulate runoff better, or worse, than the traditionally calibrated models the first days next to an updating of SCA and runoff.

4.2 SCA data evaluation, selection and conversion

Evaluation and selection

Satellite-derived SCA data available for modelling is listed in Table 2 (calibration) and Table 3 (simulation).

Table 2 Number of EO-based SCA data for calibration (AVHRR from NVE and NR, and SAR from NORUT).

	Akslen				Sjodalsvatn				Vinde-elv			
Year	NVE	NR	Norut	Used	NVE	NR	Norut	Used	NVE	NR	Norut	Used
1997	2	7	3	**5**	2	7	5	**5**	2	5	5	**2**
1998	4	6	0	**6**	3	6	1	**5**	4	5	1	**4**
1999	4	0	0	**3**	4	0	0	**3**	4	0	0	**3**

Table 3 Number of EO-based SCA data for simulation (AVHRR from NVE and NR, and SAR from NORUT).

	Akslen				Sjodalsvatn				Vinde-elv			
Year	NVE	NR	Norut	Used	NVE	NR	Norut	Used	NVE	NR	Norut	Used
1995	5	11	0	**9**	5	9	0	**10**				
1996	0	8	0	**8**	0	7	0	**7**				
2000	7	2	1	**7**	7	2	1	**7**				
2001	3	11	0	**6**	3	11	0	**6**				

The main outcome and results from the evaluation process were:

- NR-processed data were normally not useful for days with clouds, when the SCA were 10-30% below SCA from cloud-free acquisitions. The cloud-corrupted NR acquisitions were discarded.
- A small difference was observed between NR- and NVE-processed data. The difference was typically up to 5% with NVE-based SCA in the lower range.
- SAR-based SCA deviated with up to 25 % from optically-based SCA data. Most SAR acquisitions were discarded. The reason for this was that SCA observed by SAR did not show a decrease as expected from AVHRR and model simulations. The reason for this may be the procedure used for classification of dry snow by SAR.

SCA conversion

The selected SCA timeseries were processed in order to conform with the HBV-model SCA. The Akslen and Sjodalsvatn catchments are covered by 13% and 9% glaciers. The glaciers will be covered by snow or firn even at the end of the summer every year. Thus 0% SCA could never be observed over these catchments. The snow routine in the HBV-model does not consider this effect. Based on these considerations and an analysis of snow runoff and satellite-based SCA, the lower limit for SCA observation was estimated to 10% for Akslen and 5% for Sjodalsvatn. Furthermore, the HBV-model simulates 100% SCA during most of the winter before significant snowmelt starts. The satellite-based SCA observations hardly exceed 75%, and the higher limit was estimated to 75%. Based on these SCA ranges, satellite-based SCA was transformed linearly to cover the interval 0-100% before used in model calibration.

SCA comparison

SCA was retrieved form a near simultaneous set acquisitions by AVHRR, MODIS, SAR and ETM+. The ETM+ image was used as reference, as due to the high spatial resolution and proven capability to separate bare ground and snow. A data comparison was prepared by NR (AVHRR and MODIS) and Norut (SAR). In addition a comparison of the SCA from the different sensors was done by NVE in order to compare the data as they are used as input to the hydrological model.

The Landsat ETM+ image from 4 May 2000 was classified into percent SCA by NR (see Koren and Solberg 2002). The NOAA AVHRR image from 4 May 2002 was classified into percent SCA using the NVE retrieval algorithm. In addition, a linear transformation was applied that was specific to each catchment in order to transform the SCA into the range simulated by the model (0-100 %). The ERS SAR image from 3 May 2002 was classified into percent SCA by Norut (see Malnes and Guneriussen 2002). The mask applied to the SAR image was applied to all data sets in order to enable direct comparison. Figure 9 shows the SCA maps produced by the three sensors ETM+, AVHRR and SAR.

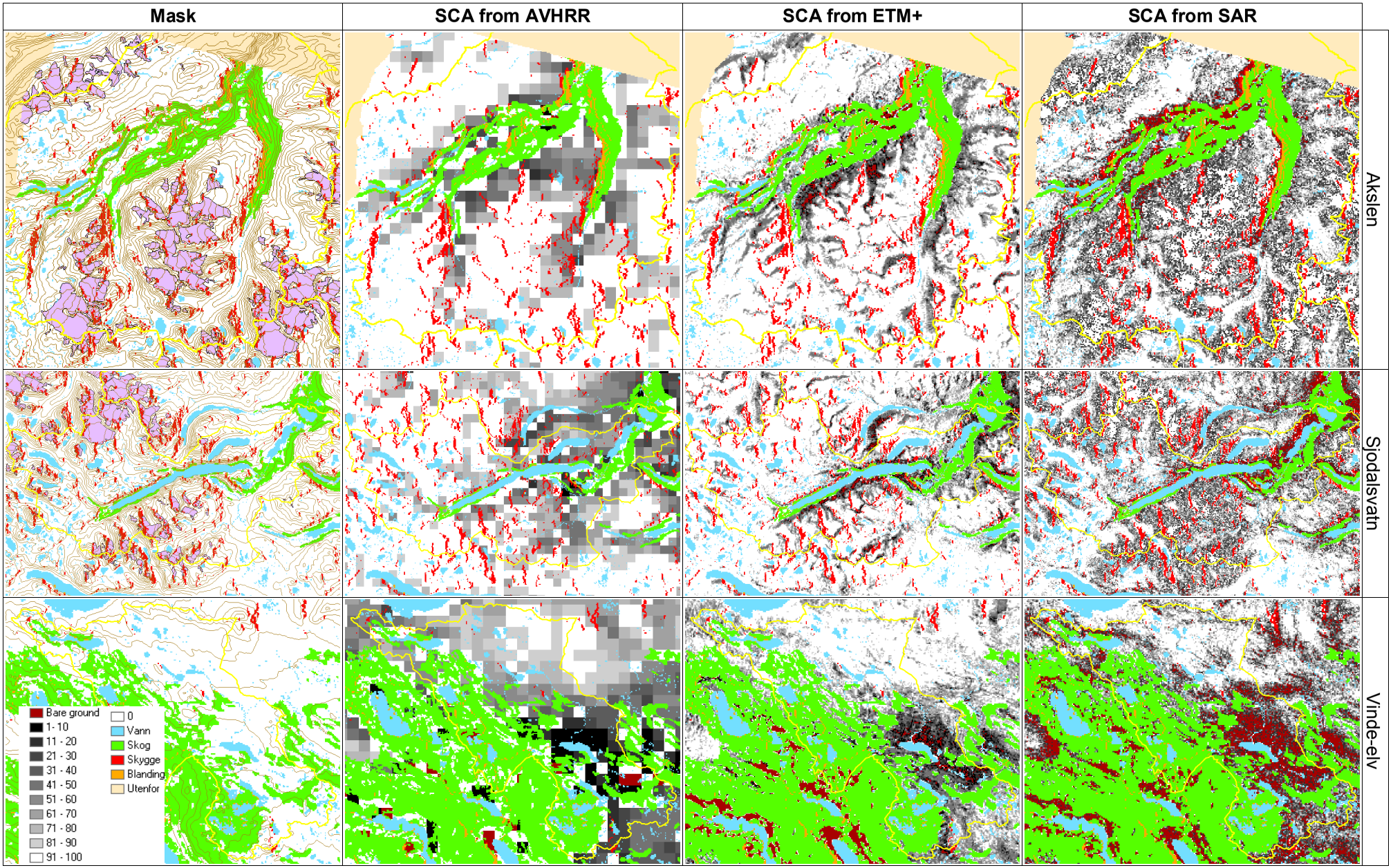

Figure 9 SCA maps for Akslen (top), Sjodalsvatn (middle) and Vinde-elv (bottom) based on data from ETM+ (left), AVHRR (middle) and SAR (right). Mask is shown to the left.

The average SCA over the unmasked areas was calculated for each of the three test catchments. The results show that the catchments were partly covered by dry snow, which called for special care when processing the SAR image. A very small part of the unmasked area was covered by 100% bare ground. In other words, most of the unmasked part of the catchment was covered by fragmented snow, which partly was dry. The results are listed in Table 4.

Table 4 Comparison of SCA calculated from different sensors on 3 and 4 May 2000.

	Total area	Unmasked area		SCA of unmasked area (%)		
Catchment	km^2	%	km^2	AVHRR	ETM+	SAR
Akslen	791	71.0	562	82.2	84.3	69.1
Sjodalsvatn	474	77.5	367	77.8	83.2	68.9
Vinde-elv	268	59.5	159	47.4	68.7	49.5

The three catchments cover an area of 1533 km^2, of which 1088 km^2 was included in the comparison as it was not masked in the SAR analysis. In terms of size, the snow covered area was 889 km^2 according to ETM+, 823 km^2 according to AVHRR, and 720 km^2 according to SAR. The study of the other dates with satellite-based SCA data suggest that the difference between optical and SAR based SCA can be even larger. The is probably due to the problem SAR has with detecting dry snow, and that a logical rule has to be applied to determine which pixels covers dry snow and also the SCA value for these pixels.

4.3 Model calibration

The three years 1997, 1998 and 1999 were used for calibration. The models were automatically calibrated using PEST. 96 models were calibrated against runoff only (called the ***Q-models***), and 96 against both runoff and SCA (called the ***QS-models***). The calibration of many models thus produced a large number of models that could be used to simulate the water balance in the catchments. In order to further select the best models three procedures were explored:

Selection A: Selection of the *Q-models* that best reproduced runoff and at the same time did not match the satellite-observed SCA well. This selection represented models that simulate runoff well and could typically be chosen for use by the flood forecasting service if SCA data was not available. Runoff only was used in the calibration.

Selection B: Selection of the *Q-models* that best reproduced runoff and at the same time matched the satellite-observed SCA well. This selection represents models that simulate runoff well and would typically be chosen for use by the flood forecasting service if SCA data was available. Runoff only was used in the calibration. Satellite-observed SCA was used to select those models that best simulated SCA.

Selection C: Selection of the *QS-models* that best reproduced runoff and SCA well. This selection represents models that simulate runoff well and could typically be chosen for

use by the flood forecasting service if SCA data was available. Both runoff and SCA were used in the calibration.

Selection A represented models that traditionally could be selected for use in the flood forecasting service or for runoff simulations. On the other hand, Selections B and C represented model that could be selected if satellite-derived SCA was available - either for calibration (Selection C) or for selection (selection B).

The results suggested that the methods used for Selection B and Selection C could be used for producing models that are better than the traditional method (exemplified by Selection A). That the difference in the results from Selection B and Selection C was small, and in the following section results from Selection A (labelled Using runoff only) and Selection C (labelled Using both runoff and SCA) are shown.

It should be noted that in this (*Model calibration*) and the next (*Model simulation*) section, the graphs showing simulated SCA (labelled *Q_SCA* in the figures) have been inversely scaled as to be comparable with the new calibration procedure used for AVHRR SCA retrieval. This means that where the graph shows a simulated SCA of 75% this is equal to 100% in the model.

Akslen

20 calibration solutions gave R^2 from 0.88 to 0.85 for the *QS-models*, and 53 solutions gave R^2=0.89 using the *Q-models*. Figure 10 shows Selection A (left) and Selection C (right) models.

Using runoff only | **Using both runoff and SCA**

1997

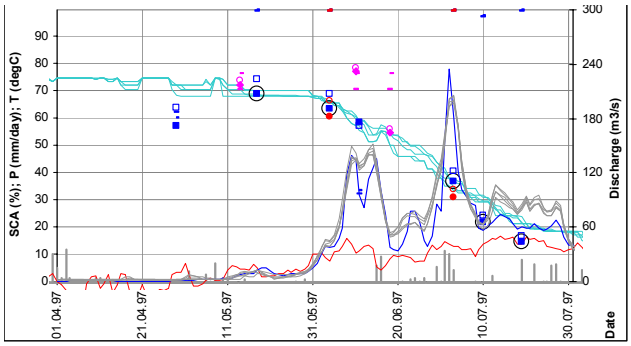

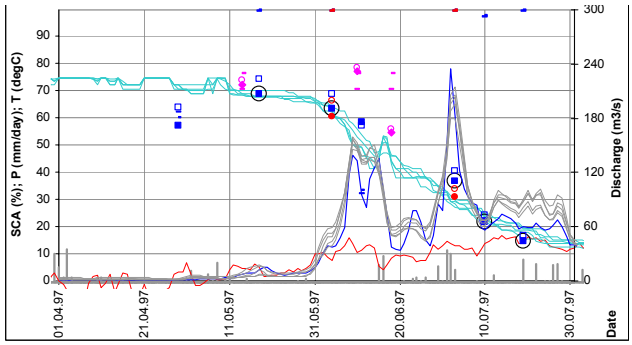

1998

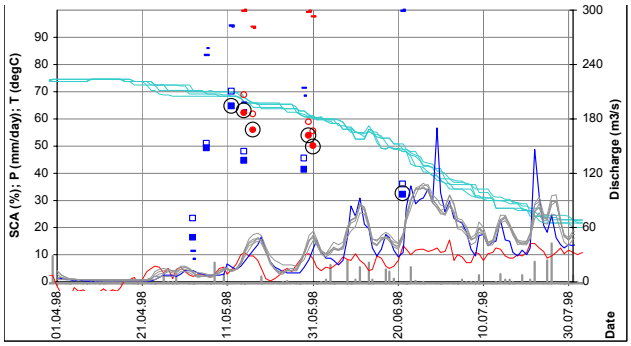

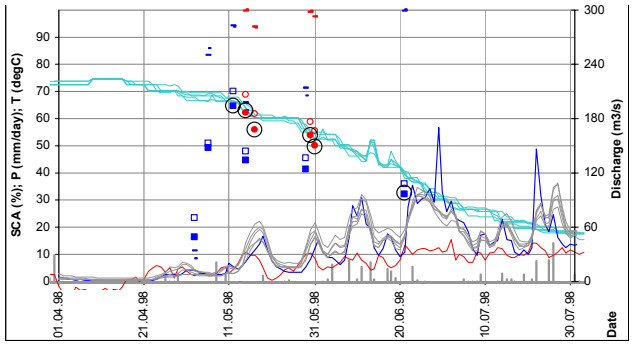

1999

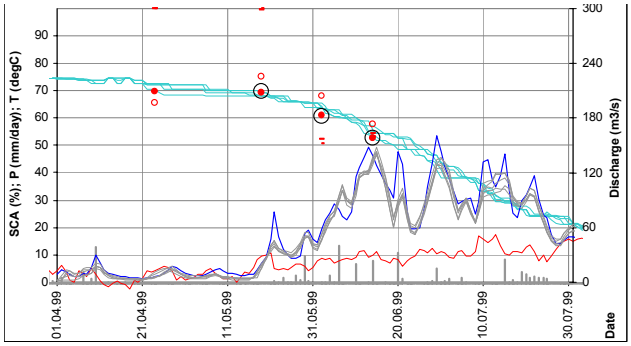

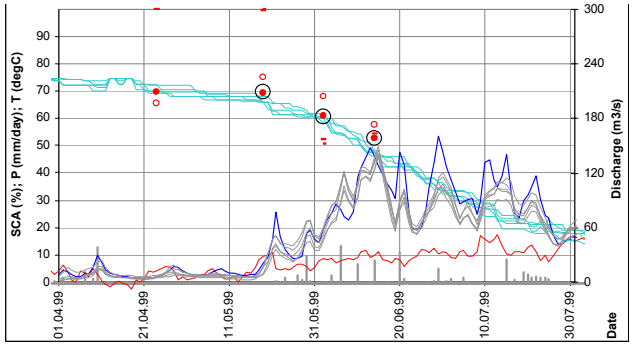

Abbreviations are as follows:
nve denotes NVE-processed images, *nr-kl* denotes NR-processed class-based images, *nr-pr* denotes NR-processed percent-based images, *rad* denotes NORUT-processed radar (SAR) images, *lan* denotes NR-processed Landsat image. *skyfr* denotes percent of catchment where SCA is calculated. *%* denotes SCA percent and *sf* denotes SCA calculated for area above treeline only. QS_Q denotes simulated runoff, QS_S simulated SCA. Q denotes observed runoff, P observed precipitation, and T temperature.

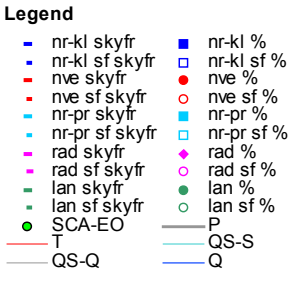

Figure 10 Calibration period Akslen catchment. The graphs show observed precipitation (P), temperature (T), runoff (Q) and SCA, and modelled runoff (HBV_Q) and SCA (HBV_SCA). The observed SCA values used in the calibration are marked with a circle.

Sjodalsvatn

15 calibration solutions gave R^2 from 0.74 to 0.75 for the *QS-models*, and 9 solutions gave R^2=0.79 using the *Q-models*. Figure 11 shows Selection A (left) and selection C (right) models.

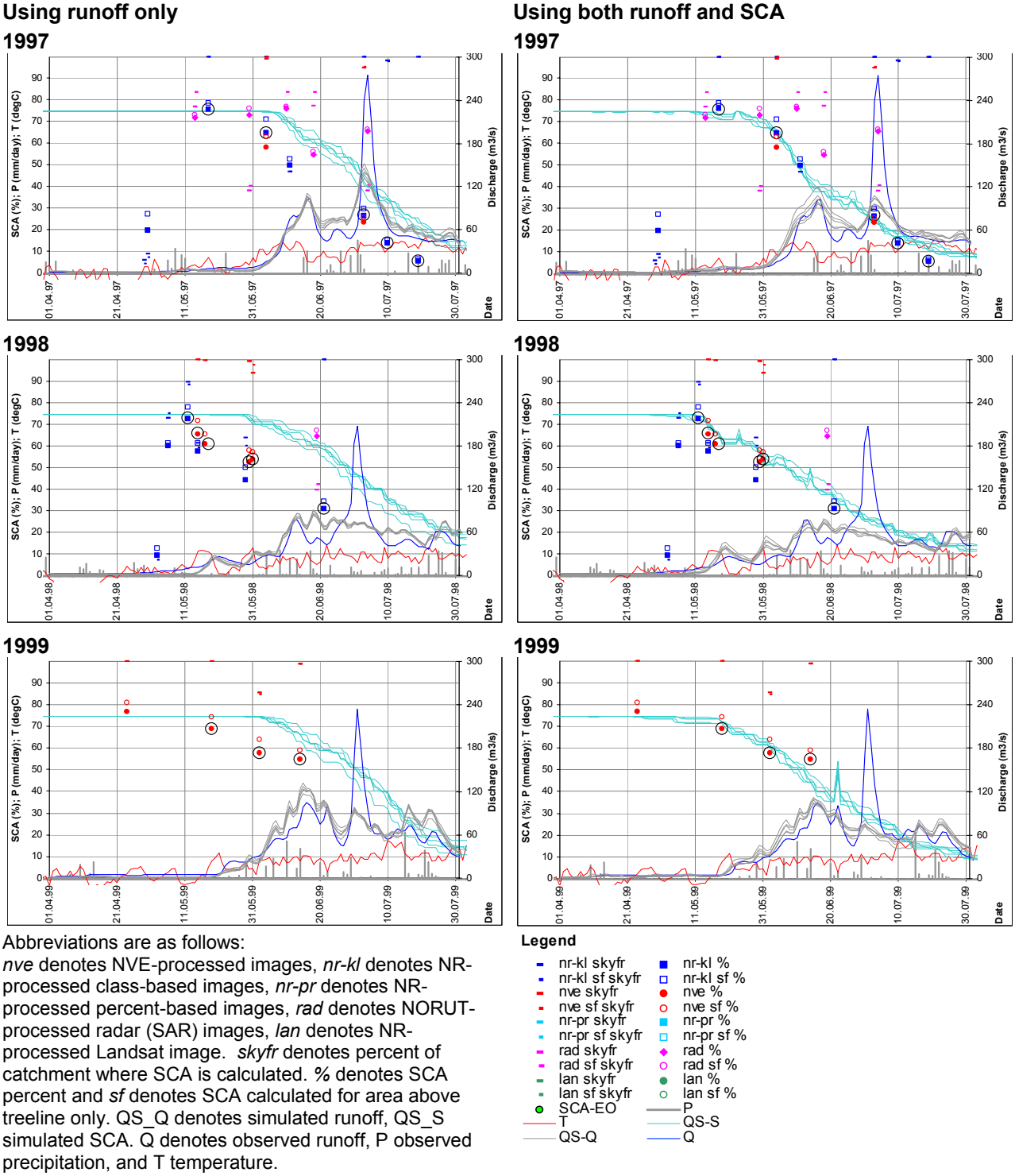

Abbreviations are as follows:
nve denotes NVE-processed images, *nr-kl* denotes NR-processed class-based images, *nr-pr* denotes NR-processed percent-based images, *rad* denotes NORUT-processed radar (SAR) images, *lan* denotes NR-processed Landsat image. *skyfr* denotes percent of catchment where SCA is calculated. *%* denotes SCA percent and *sf* denotes SCA calculated for area above treeline only. QS_Q denotes simulated runoff, QS_S simulated SCA. Q denotes observed runoff, P observed precipitation, and T temperature.

Figure 11 Calibration period Sjodalsvatn catchment. The graphs show observed precipitation (P), temperature (T), runoff (Q) and SCA, and modelled runoff (HBV_Q) and SCA (HBV_SCA). The observed SCA values used in the calibration are marked with a circle.

Vinde-elv

The upper four elevation intervals (40% of the area) above the treeline were used for calibration to avoid the SCA observation problem over forest. 14 calibration solutions gave R^2 from 0.83 to 0.81 for the *QS-models*, and 16 solutions gave R^2=0.85 using the *Q-models*. Figure 12 shows Selection A (left) and selection C (right) models.

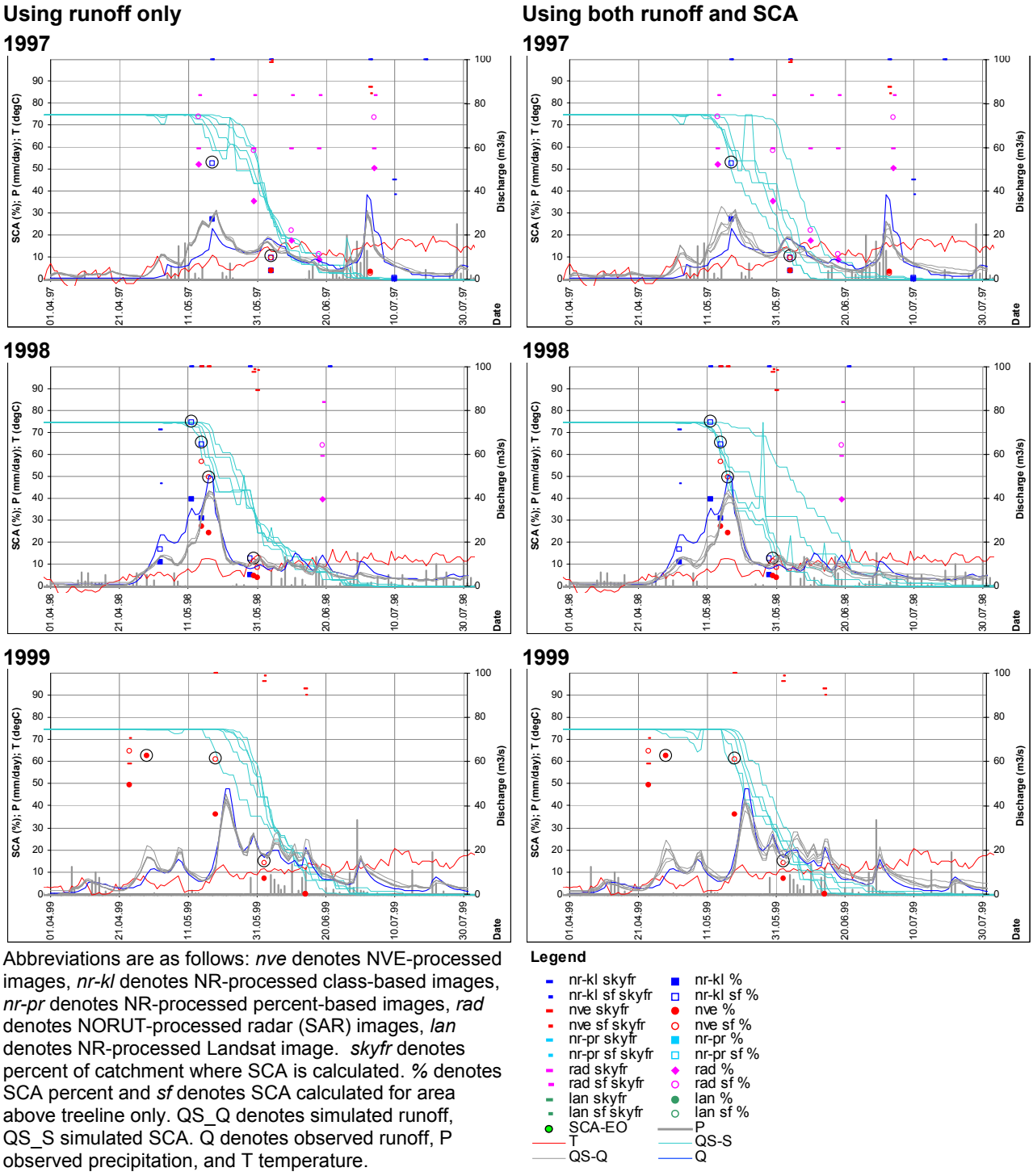

Abbreviations are as follows: *nve* denotes NVE-processed images, *nr-kl* denotes NR-processed class-based images, *nr-pr* denotes NR-processed percent-based images, *rad* denotes NORUT-processed radar (SAR) images, *lan* denotes NR-processed Landsat image. *skyfr* denotes percent of catchment where SCA is calculated. *%* denotes SCA percent and *sf* denotes SCA calculated for area above treeline only. QS_Q denotes simulated runoff, QS_S simulated SCA. Q denotes observed runoff, P observed precipitation, and T temperature.

Figure 12 Calibration period Vinde-elv catchment. The graphs show observed precipitation (P), temperature (T), runoff (Q) and SCA, and modelled runoff (HBV_Q) and SCA (HBV_SCA). The observed SCA values used in the calibration are marked with a circle.

The automatic calibration procedure finds the optimal parameter sets based on the fit between observed and simulated runoff. This implies that the model cannot be calibrated to give a better fit, using the same input data, when more variables are used. In this project the SCA variable was used in addition to runoff.

The calibration showed that SCA was simulated well by the *QS-models* without significant reduction in the quality of the runoff simulations as compared to the *Q-models*. In the Akslen case, even the *Q-models* simulated SCA well. In the cases of Sjodalsvatn and Vinde-elv, the *Q-models* clearly overestimated SCA. For this reason the *QS-models* were used to evaluate simulated SCA in the validation periods. Both the *Q-models* and *QS-models* simulated runoff well for the Vinde-elv and Akslen catchments. However, the largest floods in Sjodalsvatn were not well simulated by any of the models. The reason is probably that the point observations of precipitation and temperature at the meteorological stations do not represent the area value of the catchments during these events.

The snowmelt contribution to runoff was simulated reasonable well for the calibration years.

4.4 Model simulation

Simulations for the four years 1995, 1996, 2000 and 2001 were validated against observed runoff and SCA. The simulation results are shown in Figure 13, Figure 14 and Figure 15. Models that simulated both SCA and runoff well in the calibration were used in the validation (Selection C models, see description in the above section).

The results show that the simulation of runoff and SCA during the validation years was of the same quality as in the calibration period, which indicated that the models were consistent in time. All years except 2001 simulated SCA well for Akslen and Sjodalsvatn. For Vinde-elv, the observed SCA showed variation, which was difficult to explain. In this catchment the SCA was calculated for 40% of the area only. This made validation difficult for Vinde-elv.

Runoff was simulated fairly well for Vinde-elv and Akslen, except in 2001. The year 2001 was an exception, as none of the models performed well this year in terms of both runoff and SCA. During the autumn and winter 2000-01 extreme amounts of precipitation were recorded in south-east Norway. The ratio between precipitation at the meteorological stations and precipitation integrated over the catchments was probably not normal in during this period. The observed precipitation used as input to the model, and consequently the modelled SWE for Sjodalsvatn and Akslen were therefore probably underestimated. Such an underrating of the amount of snow in the model caused the modelled SCA to decrease too quickly when melting occurred. Another consequence was that the simulated runoff caused by snowmelt was too low throughout the melting season. For Vinde-elv the runoff simulation in 2001 tended to be too high, possibility due to an overestimation of the precipitation during the snow accumulation period.

Akslen

1995

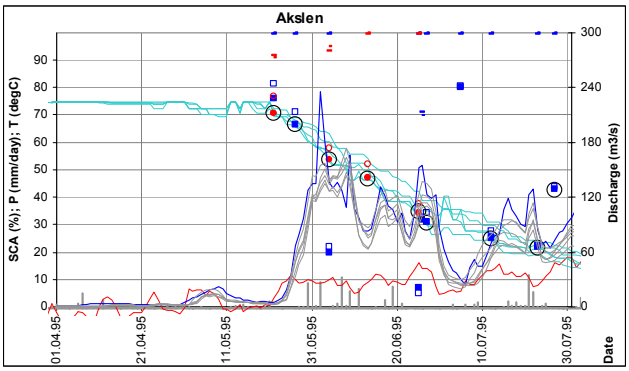

1996

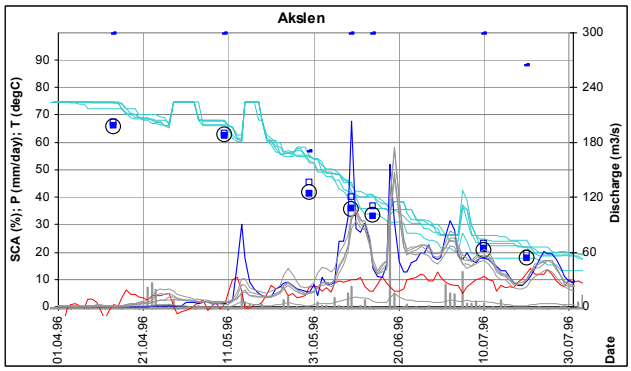

2000

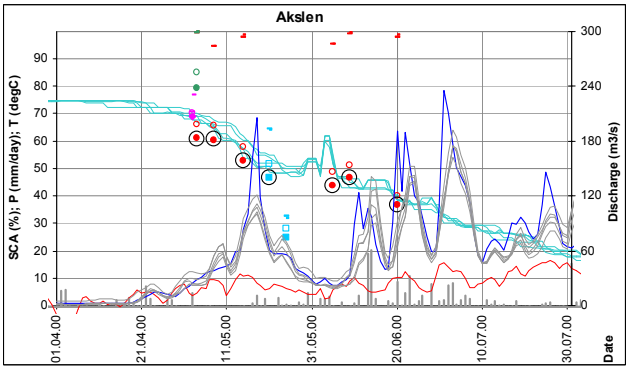

2001

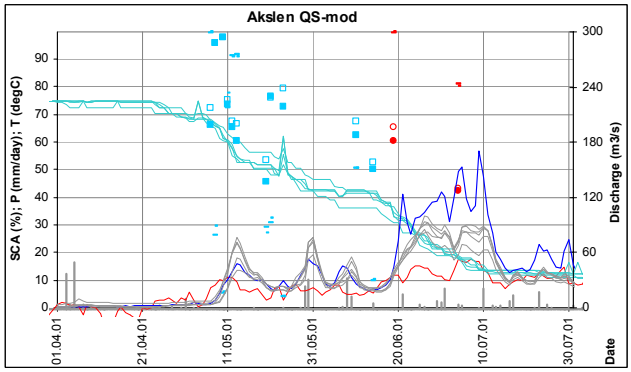

Abbreviations are as follows:
nve denotes NVE-processed images, *nr-kl* denotes NR-processed class-based images, *nr-pr* denotes NR-processed percent-based images, *rad* denotes NORUT-processed radar (SAR) images, *lan* denotes NR-processed Landsat image. *skyfr* denotes percent of catchment where SCA is calculated. *%* denotes SCA percent and *sf* denotes SCA calculated for area above treeline only. QS_Q denotes simulated runoff, QS_S simulated SCA. Q denotes observed runoff, P observed precipitation, and T temperature.

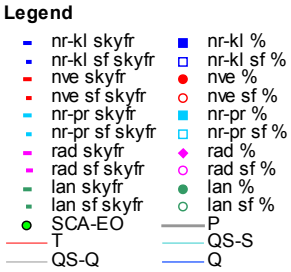

Figure 13 Simulation period Akslen catchment. The graphs show observed precipitation, temperature, runoff and SCA, and modelled runoff and SCA. The observed SCA used in the validation is marked with a circle.

Sjodalsvatn

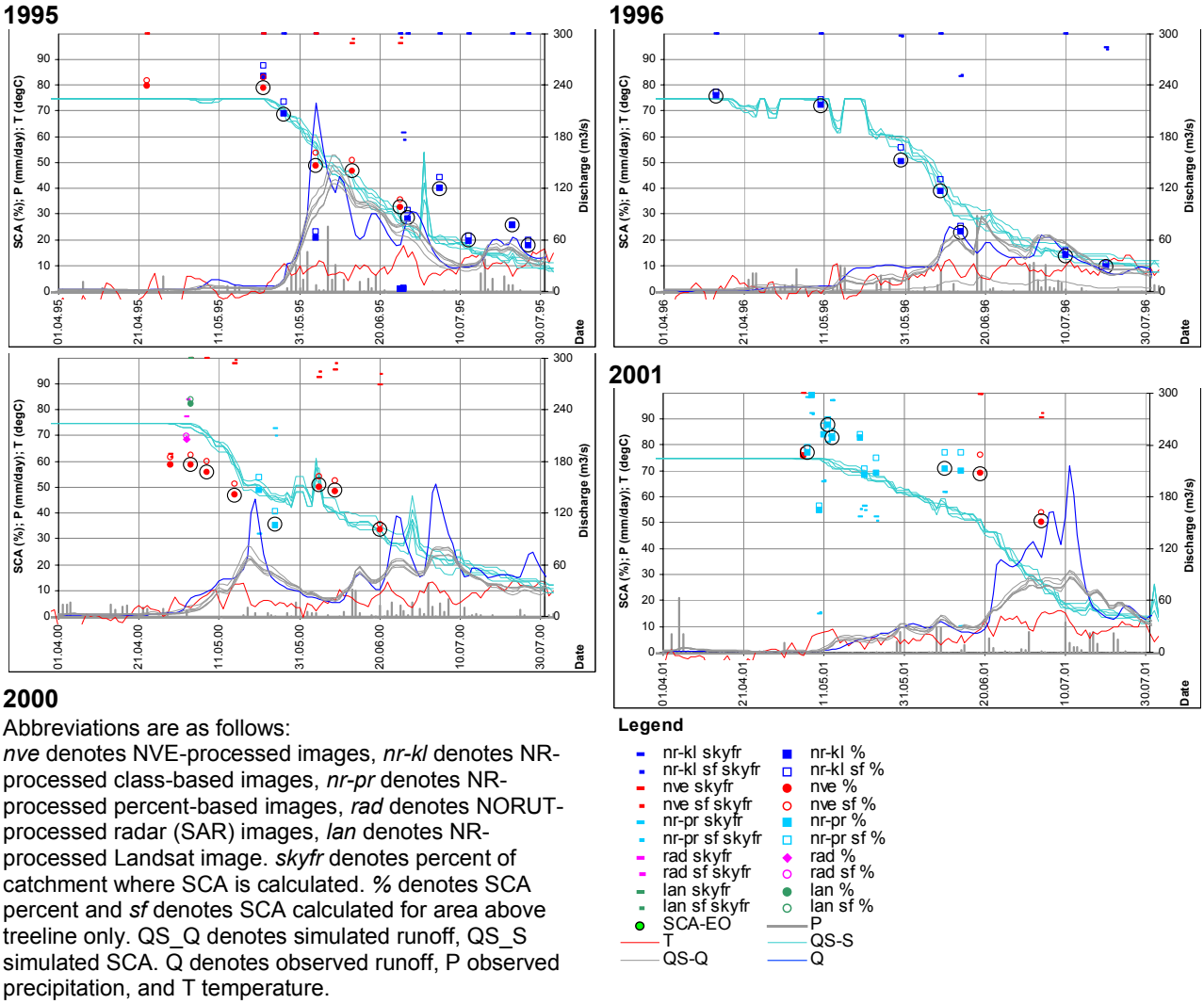

Abbreviations are as follows:
nve denotes NVE-processed images, *nr-kl* denotes NR-processed class-based images, *nr-pr* denotes NR-processed percent-based images, *rad* denotes NORUT-processed radar (SAR) images, *lan* denotes NR-processed Landsat image. *skyfr* denotes percent of catchment where SCA is calculated. *%* denotes SCA percent and *sf* denotes SCA calculated for area above treeline only. QS_Q denotes simulated runoff, QS_S simulated SCA. Q denotes observed runoff, P observed precipitation, and T temperature.

Figure 14 Simulation period Sjodalsvatn catchment. The graphs show observed precipitation, temperature, runoff and SCA, and modelled runoff and SCA. The observed SCA used in the validation is marked with a circle.

Vinde-elv

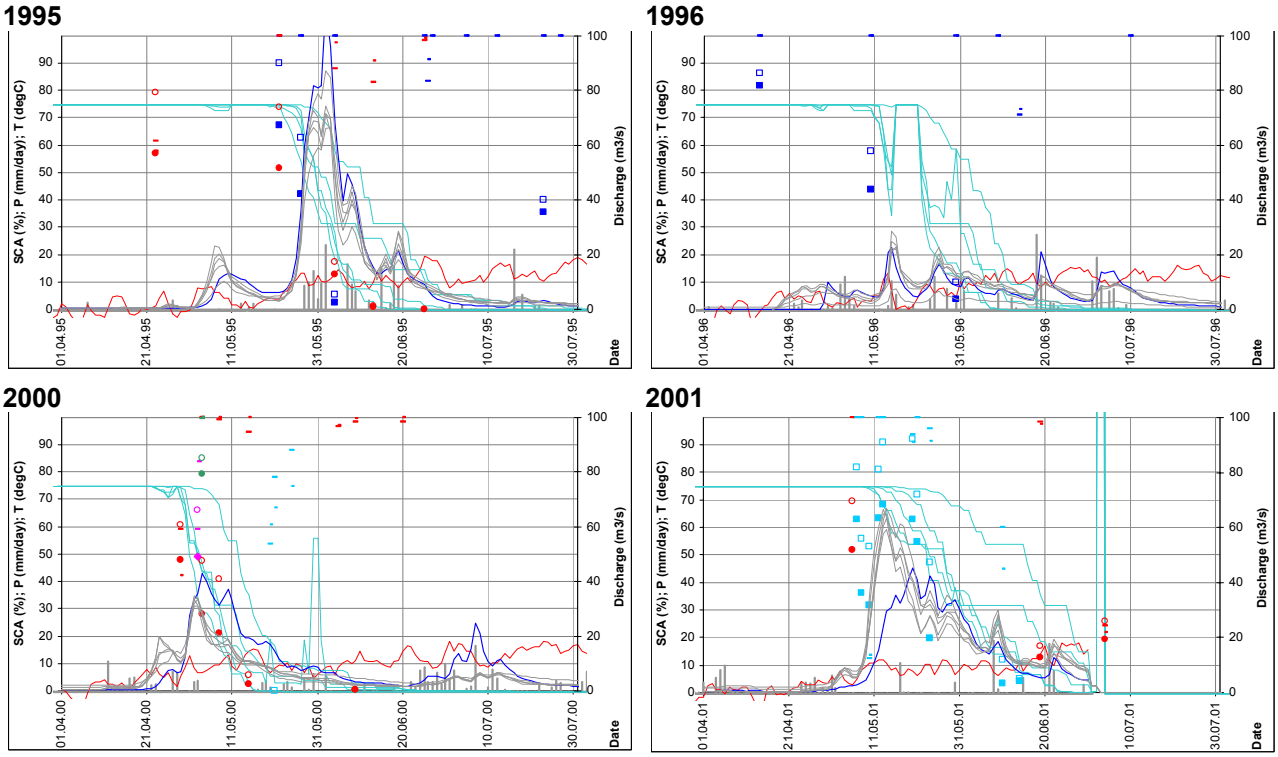

Abbreviations are as follows:
nve denotes NVE-processed images, *nr-kl* denotes NR-processed class-based images, *nr-pr* denotes NR-processed percent-based images, *rad* denotes NORUT-processed radar (SAR) images, *lan* denotes NR-processed Landsat image. *skyfr* denotes percent of catchment where SCA is calculated. *%* denotes SCA percent and *sf* denotes SCA calculated for area above treeline only. QS_Q denotes simulated runoff, QS_S simulated SCA. Q denotes observed runoff, P observed precipitation, and T temperature.

Figure 15 Simulation period Vinde-elv catchment. The graphs show observed precipitation, temperature, runoff and SCA, and modelled runoff and SCA.

4.5 Model updating

Updating of the SCA variable in the model could be done when observations and models described the same variable in a comparative way. In the HBV model, simulated SCA depend on the SWE, which has to be updated when updating SCA from observation. Two methods for updating were prescribed:

- **Input data correction:** In this method observed and simulated SCA are compared, deviation above a certain level was used to detect when the model did not manage to simulate the snow reservoir correctly. Simulated SCA and SWE were under these circumstances identified as incorrect. In order to adjust and update the model to account for this, the input precipitation and/or temperature data are adjusted to produce a better simulation. As an example, if simulated SCA decreased significantly more than observed this could be due to too little snow simulated by in the SWE variable in the model at the time of snowmelt starts at the beginning of the spring. The reason for this could be that the precipitation gauge recorded less precipitation than received in the catchment. In response to this deficiency, an increase in precipitation is applied during one day or a period of days in order to add to the snow reservoir in the model.
- **Assembly selection updating:** In this method the input data was not adjusted, but rather a new selection of calibrated models was carried out. When the SCA and SWE were incorrectly simulated, a model with a better fit between simulated and observed SCA is selected.

Model simulations showed that simulated and observed SCA and snowmelt runoff corresponded well in all years except for 2001. In 2001, simulated SCA was significantly lower than observed from the melt season started at about 10 May and until 20 June. After 20 June, the simulated runoff was only half of what was observed. For these reasons data for the catchments Akslen and Sjodalsvatn during 2001 were used for investigating the methods of model updating. The possibility and need for updating the models in the other three simulation years were assessed to be low.

4.5.1 Updating the snow reservoir by input data correction

Simulated SCA was much lower than observed on 10 June 2001, since the SWE was underestimated in the model. The divergence between modelled and observed SCA was used to detect that one or more model state variables were wrong.

The updating of the SWE in the model was done by a gradually correction of the model input precipitation before melt started in order to produce more snow in the model, and a gradual correction of temperature during the melt period in order to reduce the snow-induced runoff. Simulations using the corrected inputs were adjusted until runoff and SCA were simulated well. Simulations with and without model updating are compered to observations in Figure 16.

The five best parameter sets for simulating both runoff and SCA were used in the simulations shown in Figure 16. Updating to achieve better correspondence between

observed and simulated SCA was done until reaching a difference lower than 10% on June 10th. Both the *Q-models* and *QS-models* performed better after the updating was introduced, supporting that the proposed updating method could be successfully applied this year - simulating both flood peaks and volumes better.

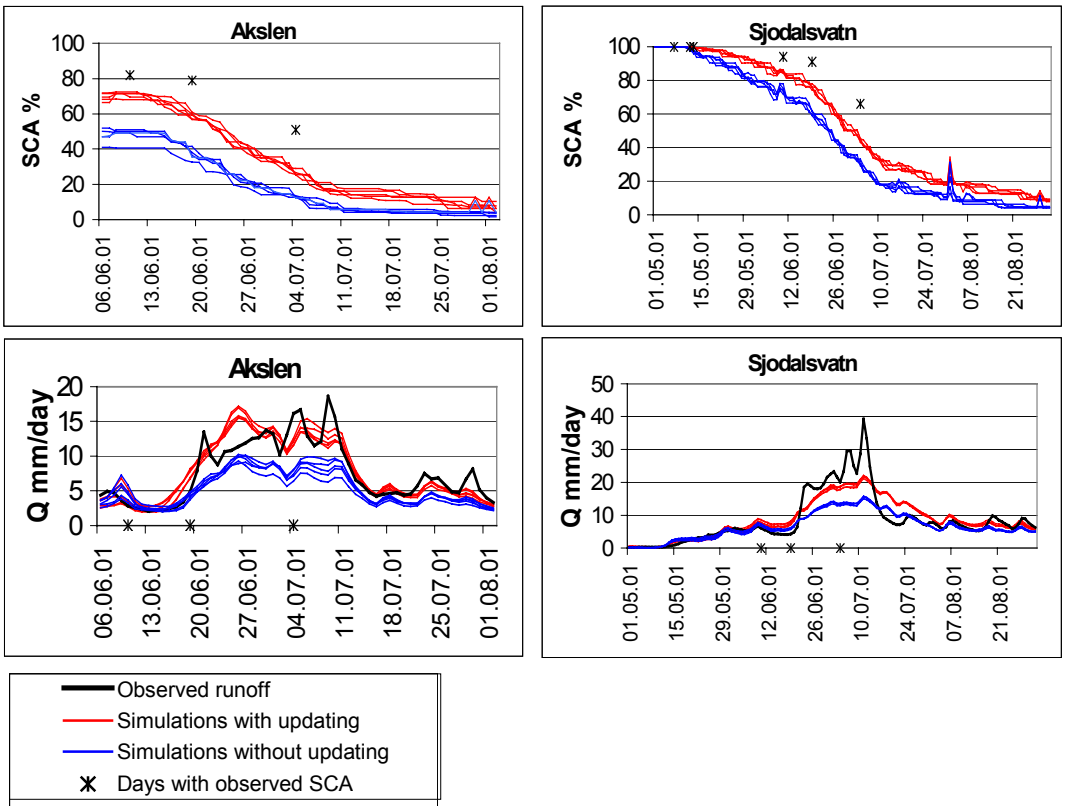

Figure 16 Simulation of SCA and runoff compered with observation for Akslen and Sjodalsvatn in 2001 with and without updating of input data to the model. The models shown are *QS-models*.

4.5.2 Updating using assembly selection

The second method for updating the model SCA was to choose the models among the *QS-models* that simulated SCA best whenever observations of SCA were available. This method was described and tested during the pilot phase of this project (Udnæs et al., 2002). The results of this method used on the 2001 data for Sjodalsvatn and Akslen are shown in Figure 17. The simulation of the updated models was compared to the best *Q-models* (the best runoff models in the calibration period).

The updating by this method appeared to give small changes in the simulations as compared to the simulations without updating for Akslen. For Sjodalsvatn this method produced poorer simulations than using the best *Q-model* without updating. Even the *QS-models* simulating SCA best did not simulate SCA well this year (Figure 17). These results suggested that the best updating method would be adjusting the input data as described in the previous section.

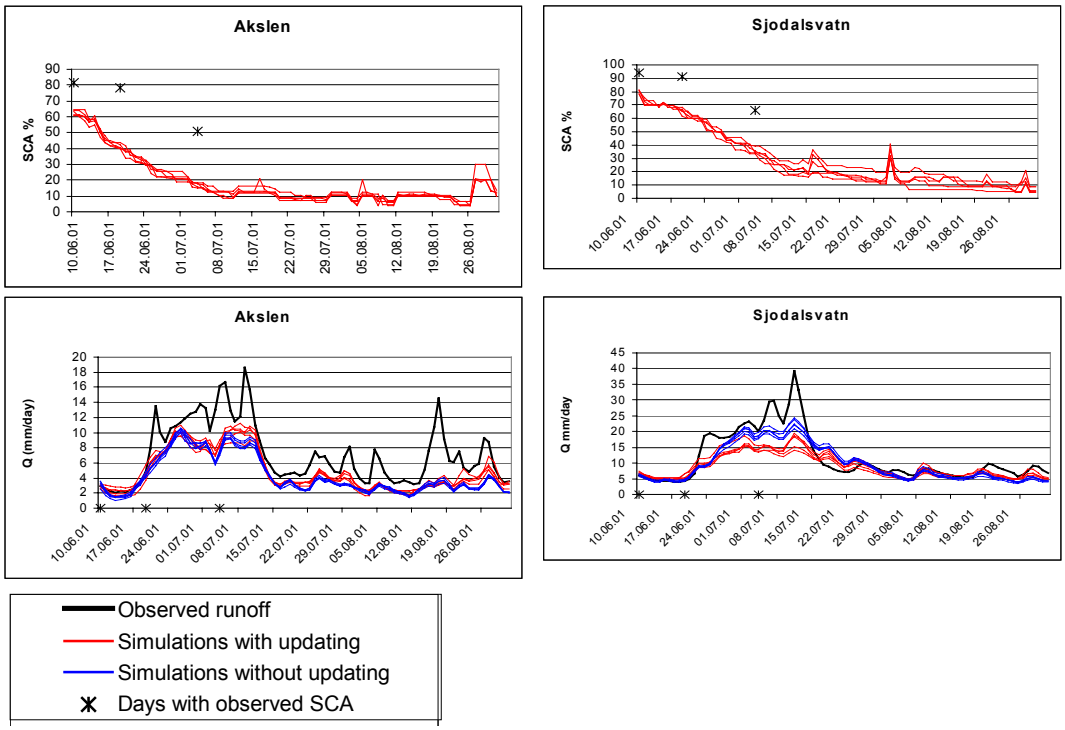

Figure 17 Simulations of SCA and runoff compared to observations for Sjodalsvatn and Akslen in 2001 with and without updating by assembly set selection. *QS-models* are shown.

5 Demonstration

A demonstration was carried out for Akslen during the period from 1 September 2001 to 1 August 2002. The results are shown in Figure 18. It should be noted that the meteorological input data used for the demonstration had not been subjected to final quality control at *met.no* - as is the case for all data used in the day-to-day flood forecasting.

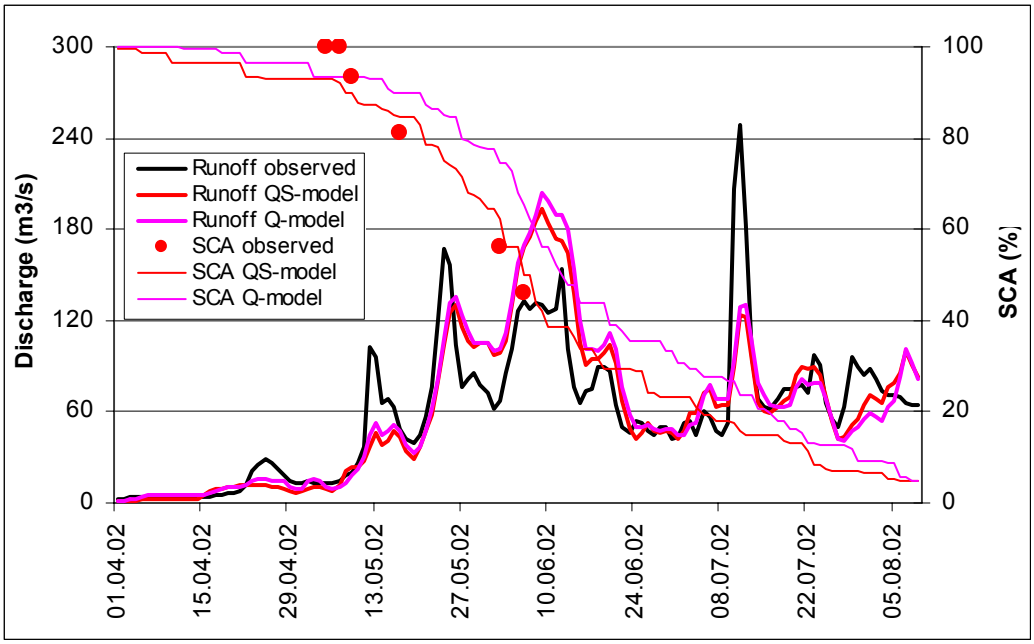

Figure 18 Results from Akslen during the demonstration period.

Simulated SCA (*QS-model* in the figure) was in fair agreement with satellite observations, which suggested that model updating was not required. The correlation between simulated and observed runoff was lower this year than all other years except 2001. Simulated runoff was consistently higher than observed for a period of four weeks from the end of May until the end of June. This situation was the reverse of that identified in 2001. In 2001, simulations showed much lower runoff than observed and this was attributed unobserved or underestimated precipitation, which produced a too small snow reservoir in the model at the time of snow maximum. In 2001, the problem was identified as a problem with the snow simulation since observed SCA was much higher than simulated. However, in 2002 the observed SCA was in accordance with simulated. With the existing methods and data we could not use the SCA to correct and update the model in order to simulate runoff better during this period.

Figure 18 also shows the results from an example of a model, which simulated runoff well and SCA less well in the calibration period (*Q-model* in the figure). This model overestimated SCA with more than 20% during long periods. This model could hardly been used to detect errors in the simulated SCA and the snow reservoir.

6 Conclusions

The results showed that the HBV-model could be calibrated against SCA in addition to runoff and simulate SCA well without major reduction in the precision of the runoff simulations. In order to this, the calibration of the SCA retrieval algorithm had to be changed. The satellite-observed SCA provided a new and independent mean to assess how well the HBV-model simulated the snow reservoir. This was used to detect when the model did not simulate the snow reservoir correctly. When such simulation errors were identified, promising results were found by updating the model by correcting the input temperature and precipitation data. Another method of model updating, updating by selecting the best model whenever a SCA observation was available did not improve the simulations as initially suggested in the pilot study.

Uncertainties were identified in the precision of the satellite-derived SCA. Further work should aim at producing time- and sensor-independent SCA estimates in order to calibrate and verify the model results against consistent data. The gap between SAR and optically based SCA observations was not systematic and at times too large. Methods for estimating SCA in sparsely forested areas are also required. This study suggests that the precision of the SCA observation for a catchment should be better than 10%. To assess the model simulation of the snow reservoir and snowmelt, a series of observations are required. If the uncertainty in observed SCA is low, two or three acquisitions during the melt period are sufficient to assess if the model simulates snow well. If the uncertainty is high, more acquisitions are required.

The HBV-model has a simplified description of the snow, groundwater and lake reservoirs. Few of the state variables are directly observable. We have through this project shown that it could be useful to observe the state variable SCA by satellite in order to assess the model simulation. However, the simulated runoff will always deviate from observed, due to the simplified structure of the model, the lack of observations of other state variables and the difference between point observations and catchment values of precipitation and temperature. The results showed that the choice of catchment and study years gave different results, which suggest that more study catchments and years should be included to achieve more general conclusions.

7 References

Brebber, L., Doherty, J. and Whyte, P., 1994. PEST – Model Independent Parameter Estimation. Watermark Computing, Corinda, Australia.

Malnes, E., and Guneriussen, T., 2002. Demosnø - Algorithms for mapping snow covered area with SAR. Norut IT Report 670/1-02.

Koren, H., and Solberg, R., 2002. DemoSnow - Snow cover mapping with optical data. Norsk Regnesentral Note SAMBA/24/02.

Riggs, G.A., Hall, D.K., and Salomonsen, V.V., 1996. Recent Progress in development of the Moderate Resolution Imaging Spectrometer snow cover algorithm and product. IGARSS'96 Conference Proceedings, Lincoln, NE, pp. 139-141.

Schjødt-Osmo, O., and Engeset, R., 1997. Remote sensing and snow monitoring: Application to flood forecasting. In Operational Water Management, Refsgaard, J.C., and Karalis, E.A. (eds). Proc. European Water Resources Association Conference, 3-6 September 1997, Copenhagen, Denmark.

Nagler T., and Rott, H., 2000. Retrieval of wet snow by means of multitemporal SAR data. IEEE Trans. Geoscience and remote sensing, 38(2), 754-765.

Solberg, R., and Andersen, T., 1994. An automatic system for operational snow-cover monitoring in the Norwegian mountain regions. IGARSS'94 Conference Proceedings. Pasadena, California August 8-12 1994.

Udnæs, H.-C., Engeset, R.V., and Andreassen, L.M., 2002. Use of satellite-derived snow data in a HBV-type model. Proceedings of the Workshops of EARSeL Special Interest Groups: Remote Sensing of Land Ice and Snow, 11-13 March 2002, Bern, Switzerland.

8 Annexes

Annex 1: NVE's paper presented to the EARSeL SIG Workshop in Bern, Switzerland, 11-13 March 2002: Remote Sensing of Land Ice and Snow.

Annex 2: HBV model description.

Annex 1

NVE's paper presented to the EARSeL SIG Workshop in Bern, Switzerland, 11-13 March 2002: Remote Sensing of Land Ice and Snow.

USE OF SATELLITE-DERIVED SNOW DATA IN A HBV-TYPE MODEL

Hans-Christian Udnæs, Rune V. Engeset and Liss M. Andreassen
Telephone: +47 22959595, E-mail: hcu@nve.no, Internet: www.nve.no
Address: Norwegian Water Resources and Energy Directorate, Box 5091 Maj., N-0301 Oslo, Norway.

ABSTRACT

The work reported in this paper, focuses on the use of satellite-derived snow cover area (SCA) data in the precipitation-runoff model, HBV. SCA is derived from optical satellite imagery to test if the hydrological model may simulate runoff better if it is calibrated using SCA data in addition to runoff. HBV models are calibrated for 3 catchments in the mountainous area in the southern Norway. Several parameter sets are calibrated automatically against runoff, and against runoff and SCA. Simulations are then carried out for a verification period. For all catchments the additional calibration against SCA caused clear improvements in simulation of SCA. For two of the catchments there was minor reductions in the precision of the runoff simulations. In the simulation period, the models calibrated against SCA and runoff did not prove to simulate runoff better, or worse, than the traditionally calibrated models the first days next to an updating of SCA and runoff. The precision of the utilised method of deriving SCA from AVHRR images is probably too low for most catchments. Operational updating of the SCA in the simulations will therefore only be of interest when there are obvious errors in the simulations.

1 INTRODUCTION

1.1 Objectives

The work reported in this paper, focuses on the use of satellite-derived snow cover area (SCA) data in the precipitation-runoff model HBV (1). SCA is derived from optical satellite imagery. The main objective is to test if the hydrological model may simulate runoff better if it is calibrated using SCA data in addition to runoff. Traditionally only runoff is used to calibrate the model.

1.2 Motivation

The amount and timing of snowmelt runoff from snow and glaciers are important information for flood prediction and hydropower operations in Norway. Satellite-based remote sensing instruments have shown to be an efficient tool for monitoring of snow parameters. The cloud cover has so far limited full operational utilisation of optical sensor products. Operational utilisation of radar data has primarily been limited by high costs. A number of hydrological models for runoff monitoring and forecasting are used throughout Europe, many of which, in principle, can be updated by earth observation data. The HBV model is used for operational forecasts in a large number of Scandinavian catchments as well as for the river Rhine in Switzerland. The model is used for flood warning, and planning, design and operation of hydropower systems, impact assessments and climate change studies. Previous works in the Snow-Tools project (2) and in the Hydalp project (3) showed that updating of HBV models, with remotely sensed data on SCA, tended to reduce the model performance. Operational use of satellite derived snow parameters in the HBV-model has not been reported and only a few authors have reported operational applications of remotely sensed snow parameters in other models (4, 3). The Norwegian Water Resources and Energy Directorate (NVE) updates HBV models on a daily basis for 63 catchments throughout Norway as part of NVEs national flood warning services. The main motivation for this work is thus to see if the national flood forecasting could be improved by using AVHRR-derived snow covered area in the operational hydrological model (5).

Other direct beneficiaries from an improved simulation of the water balance are stakeholders in the fields of hydropower production planning, distribution grid load forecasting, national electricity demands and availability forecasting and climate change issues and studies.

1.3 Framework

This research takes part in the technical and methodological development of the national flood forecasting service at NVE. Parts of the work reported in this study are carried out under the application development project DemoSnø (funded by the Norwegian Space Centre). NVE is partner in two research projects on snow remote sensing and modelling, in which scientific advances are translated into improved public services: the projects SnowMan (Norwegian Research Council funding) and EnviSnow (European 5th framework programme funding).

2 METHODS

2.1 Retrieval of snow cover area from satellite imagery

NOAA AVHRR satellite images were processed according to the method described by Schjødt-Osmo and Engeset (6). This method is based on the assumption that the bare-ground reflectance, and the reflectance of snow covered areas, are constant in space at every AVHRR-scene. Reflectance values for 100% and 0% snow cover are found from glaciers and snow-free areas. The snow cover percentage for an area is then calculated as a linear function of the reflectance in this area compared to the 100% and the 0% reflectance.

2.2 Calibration of model using discharge and snow cover area observations

The model is first calibrated against runoff data only – this is referred to as the *Q model*. The three-year period from 1.9.1996 to 1.9.1999 is used for calibration. Automatic calibration is carried out with the PEST software (7). As the HBV-model is highly over-parameterised (8, 9), standard values are assigned to some of the calibration parameters. The snow parameters allowed to be calibrated, are selected based on previous studies of similar models applied to snow pillow data in Norway (10). Secondly the model is recalibrated against both runoff and SCA data – this is referred to as the *SCA-Q model*.

2.3 Simulation

Simulations are carried out using both the Q model and the SCA-Q model. The periods from 1.9.1999 to 1.9.2000, and from 1.9.1994 to 1.9.1996 are simulated. The performance of the Q and SCA-Q models is compared based on their ability to simulate runoff. Main focus is put on assessing the simulations during high discharge periods according to the primary needs of the forecasting services.

3 DATASETS AND STUDY AREA

3.1 Study areas

Three catchments were selected as test areas (11) in the central mountain range in southern Norway (table 1). The catchments range from 268 to 791 km^2, have different elevation ranges, and are mainly located above the tree line. The location and topography of the catchments are shown in figure 1.

Table 1: Study catchments characteristics.

Catchment [water gauge ident. and name]	River	Area [km^2]	Elevation [m a.s.l.]			Runoff data period	Forested area [%]	Lake area [%]	Glacier area [%]
			Min.	Max.	Med.				
12.207 Vinde-elv	Vinde	268	560	1686	985	1919-2001	31	7	0
2.13 Sjodalsvatn	Sjoa	474	940	2400	1461	1930-2001	~5	9	9
2.268 Akslen	Bøvra	791	480	2472	1476	1934-2001	13	2	12

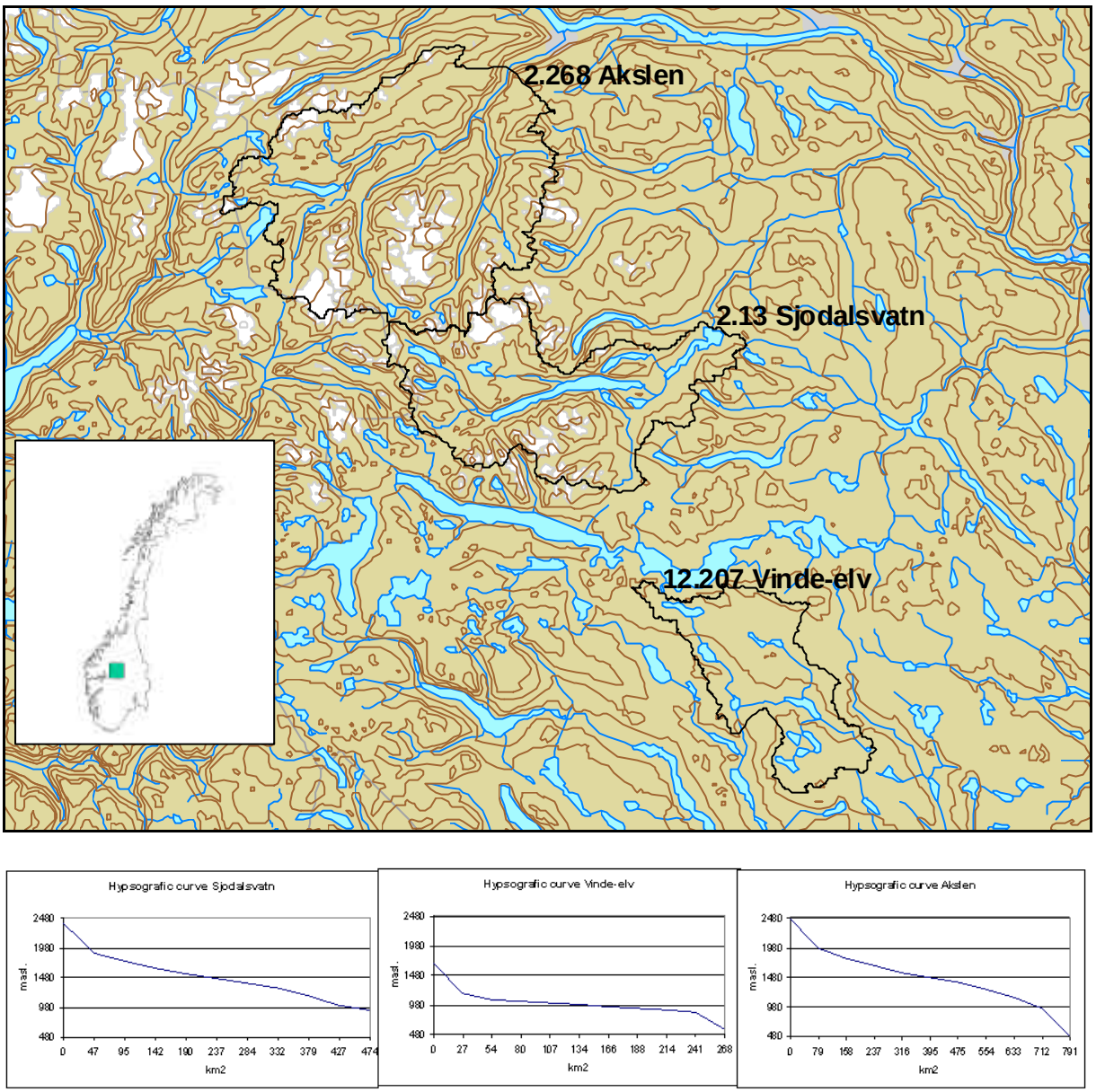

Figure 1: Map of study catchments and hypsografic curves.

3.2 Satellite image data and SCA maps

17 AVHRR images were processed to produce SCA maps of 1 km^2 resolution at the following dates: 22.5.1995, 4.6.1995, 13.6.1995, 25.6.1995, 4.6.1997, 3.7.1997, 15.5.1998, 17.5.1998, 31.5.1998, 19.5.1999, 2.6.1999, 14.6.1999, 8.5.2000, 15.5.2000, 5.6.2000, 9.6.2000 and 20.6.2000.

The SCA maps were used to calculate the total SCA for each catchment at the dates when cloud-free AVHRR data were available. The calculated SCA values are given in table 2.

Table 2: Calculated snow covered area(%) from NOAA AVHRR images

Year	**1995**				**1997**		**1998**			**1999**			**2000**				
Date	**22.5.**	**4.6.**	**13.6.**	**15.6.**	**4.6.**	**3.7.**	**15.5.**	**17.5.**	**31.5.**	**19.5.**	**2.6.**	**14.6.**	**8.5.**	**15.5.**	**5.6.**	**9.6.**	**20.6.**
Sjodalsv.	79	49	47	33	62	24	65	61	53	69	63	55	56	47	51	49	34
Vinde-elv	53	13	1	0	5	0	27	24	4	36	8	0	22	3	0	0	0
Akslen	71	54	48	35	64	31	63	56	51	70	61	53	61	53	44	47	37

3.3 Water balance, snow reservoir and floods

Discharge has been observed automatically using gauging stations at each of the study catchments. Figure 2 shows the discharge series for each catchment for the calibration years 1997-1999. Figure 3 shows the discharge series for the simulation years 1995-1996 and 2000. The major floods are dominated by snowmelt for all the catchments. The Vinde-elv catchment has usually one clearly defined melting flood yearly. This flood is mainly caused by simultaneous snow melting in most of the catchment, due to the small variations in elevation. The catchment has a relative high lake percentage, and also some more capacity of groundwater storage than the other catchments. Flooding situations, due to rain alone, do rarely occur. The other catchments, Sjodalsvatn and Akslen, will usually have more than one flooding situation yearly because snowmelt often occurs at different times in the different elevation zones. These catchments may also have considerable melting contributions from glaciers during the summer and autumn. The discharge from the Akslen catchment is to a small degree restrained by natural reservoirs, as lakes and groundwater reservoirs. In this catchment there is a fast response in runoff at most rain and melting situations. In the Sjodalsvatn catchment there are large lakes situated close to the outlet of the catchment. These lakes will store most of the melting water in the beginning of the melting period, and the largest floods will only occur after the water level in these lakes has reached a certain level. The regulating effect of the lakes is clearly illustrated by figure 2 and 3 when variations in daily discharge at Akslen and Sjodalsvatn are compared.

Based on measurements from power suppliers and simulations with the HBV model, the years 1995, 1998 and 1999 had relative, but not extreme, high amounts of snow in the actual catchments in the beginning of May. In 1996 the amount of snow seemed to be extremely low.

The largest floods in the area are usually caused by a combination of rain and snow melting. In the end of May 1995, at a time when melting normally have started below 1000 m a.s.l., the amounts of snow was considered extremely high below this altitude. A strong increase in temperature, combined with extensive rainfall, resulted in one of the largest floods in the south east of Norway in the 20th century. Large floods were also observed in the actual catchments at this occasion. In the period 1994-2001 the largest floods observed in Akslen and Sjodalsvatn occurred in the beginning of July 1997. This flood was also a combination flood of melting and rainfall.

To isolate the contribution of snow melt in a flooding situation is a difficult task because of lack in representative precipitation observations. However, some of the observed floods appear to be pure snowmelt floods, as the floods in May 1997, 1998 and 1999 in Vinde-elv. In Akslen and Sjodalsvatn all the major floods seem to be combination floods.

4 RESULTS

4.1 Calibrations

A number of parameter sets are automatically calibrated for each of the three catchments, with and without calibration against SCA in addition to runoff. For the models calibrated against runoff, the results show large deviations between HBV-simulated and AVHRR-observed SCA. The calibration uncertainty was confirmed to be large as several optimal parameter combinations gave different runoff simulations of approximately equal quality. For the models calibrated against runoff and SCA, the results show better simulations of SCA, but some reduction in the quality of the runoff simulations, particularly for one of the catchments, Vinde-elv. Results from the best calibrations are shown in table 3 and in figure 4. The quality of the runoff calibrations are measured by the R^2-value (5) where $R^2 = 1$ describes a perfect calibration. For two of the catchments, Akslen and Vinde-elv, the calibrations against runoff are fairly good, even if the simulations tend to underestimate the largest floods. The calibrations for Sjodalsvatn have lower quality, mainly in the flooding situations.

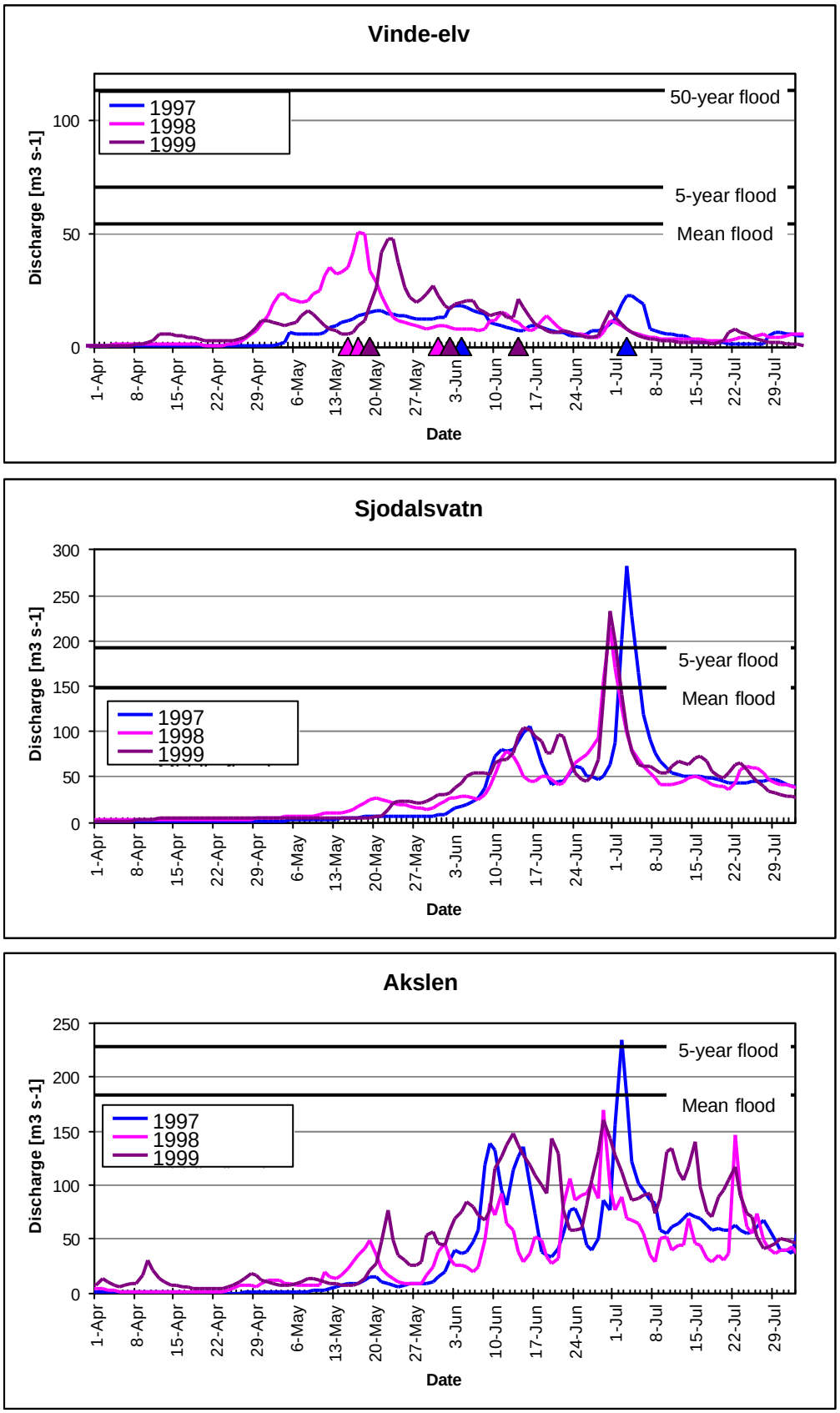

Figure 2: Discharge data during the snowmelt period (April-July) in the three years of data used in model calibration. Coloured triangles indicate available AVHRR-derived SCA maps.

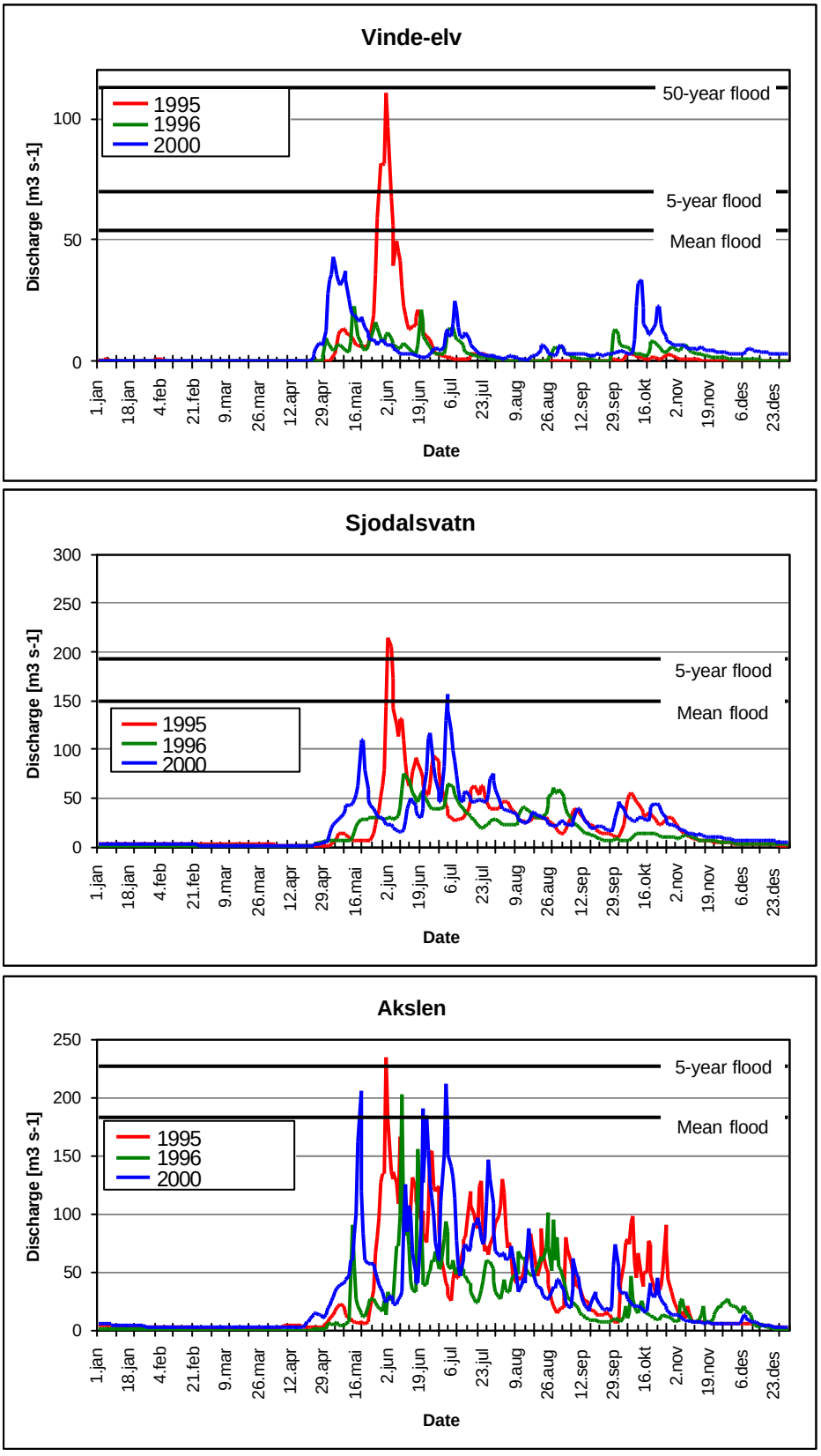

Figure 3: Discharge data in the three years of data used in model simulation.

Table 3: Simulated SCA, by Q model and SCA-Q model, compared to AVHRR-derived SCA, 1997-1999.

	AKSLEN			SJODALSVATN			VINDE-ELV		
	sim SCA Q mod %	sim SCA SCA-Q mod %	obs SCA AVHRR %	sim SCA Q mod %	sim SCA SCA-Q mod %	obs SCA AVHRR %	sim SCA Q mod %	sim SCA SCA-Q mod %	obs SCA AVHRR %
04.06.97	82	70	64	73	52	62	17	6	5
03.07.97	28	22	31	24	13	24	0	0	0
15.05.98	84	68	63	97	81	65	74	29	27
17.05.98	78	65	56	93	78	61	59	18	24
31.05.98	66	53	51	83	60	53	15	3	4
19.05.99	86	72	70	99	83	69	89	34	36
02.06.99	69	58	61	87	70	63	26	6	8
14.06.99	45	39	53	73	50	55	7	1	0
mean |sim SCA - obs SCA|	14	7		19	11		23	2	
R^2 (runoff)	0.84	0.80		0.76	0.73		0.86	0.33	

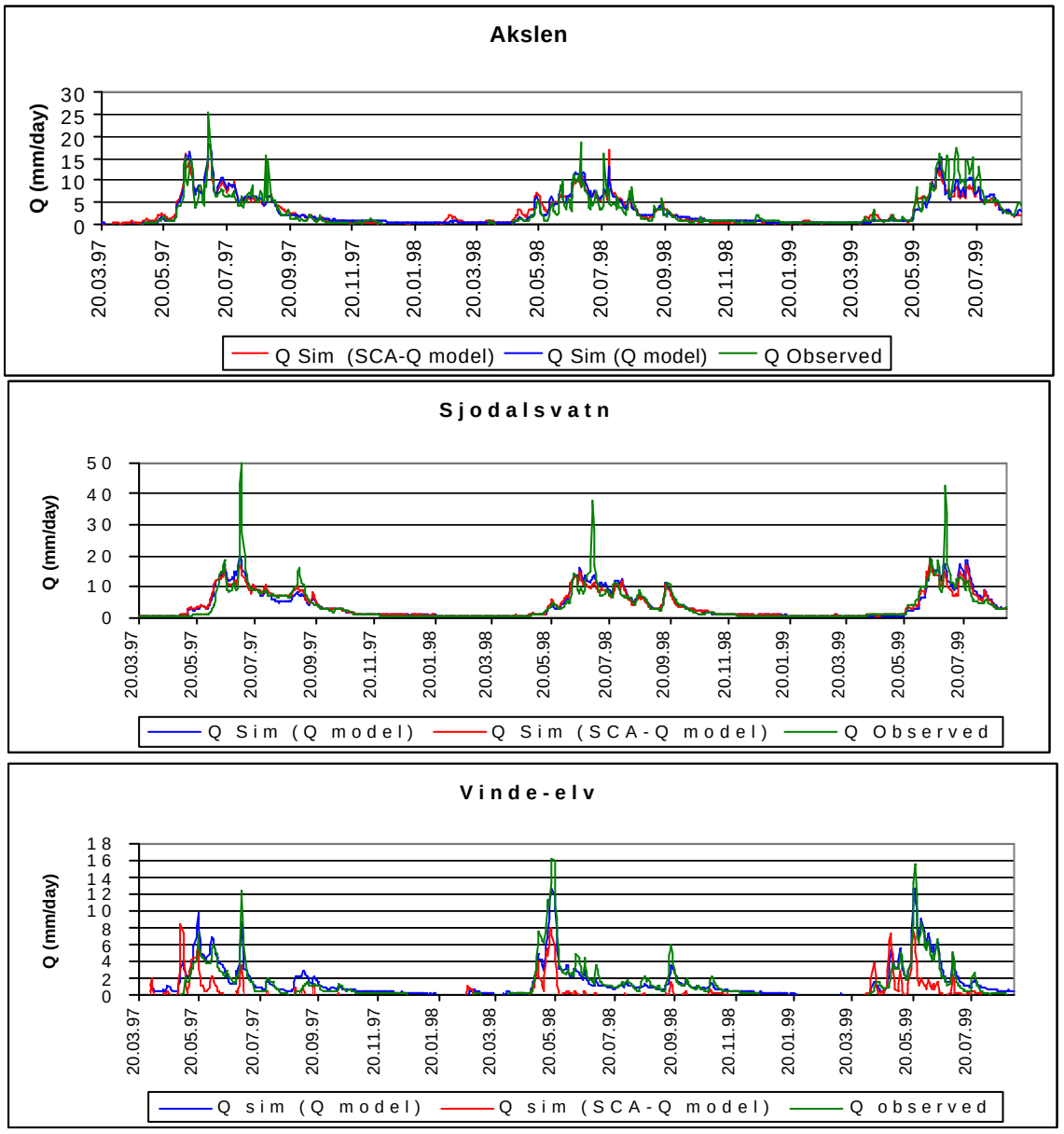

Figure 4: Simulated and observed runoff compared for the calibration period.

4.2 Simulations

Simulations, using the best parameter sets (up to 50 sets) for each catchment, are carried out for the entire period 1.9.1994-1.9.2000. Special attention is paid to the melting periods in 1995 and 2000 where simulations by Q models and SCA-Q models were updated when AVHRR data were available. At every updating the five Q models that perform best at that moment, are used in the simulations until the next updating. Likewise, the five SCA-Q models that simulate runoff best, among those who simulate SCA fairly well (AVHRR SCA +/- 5%), are used in the further simulations.

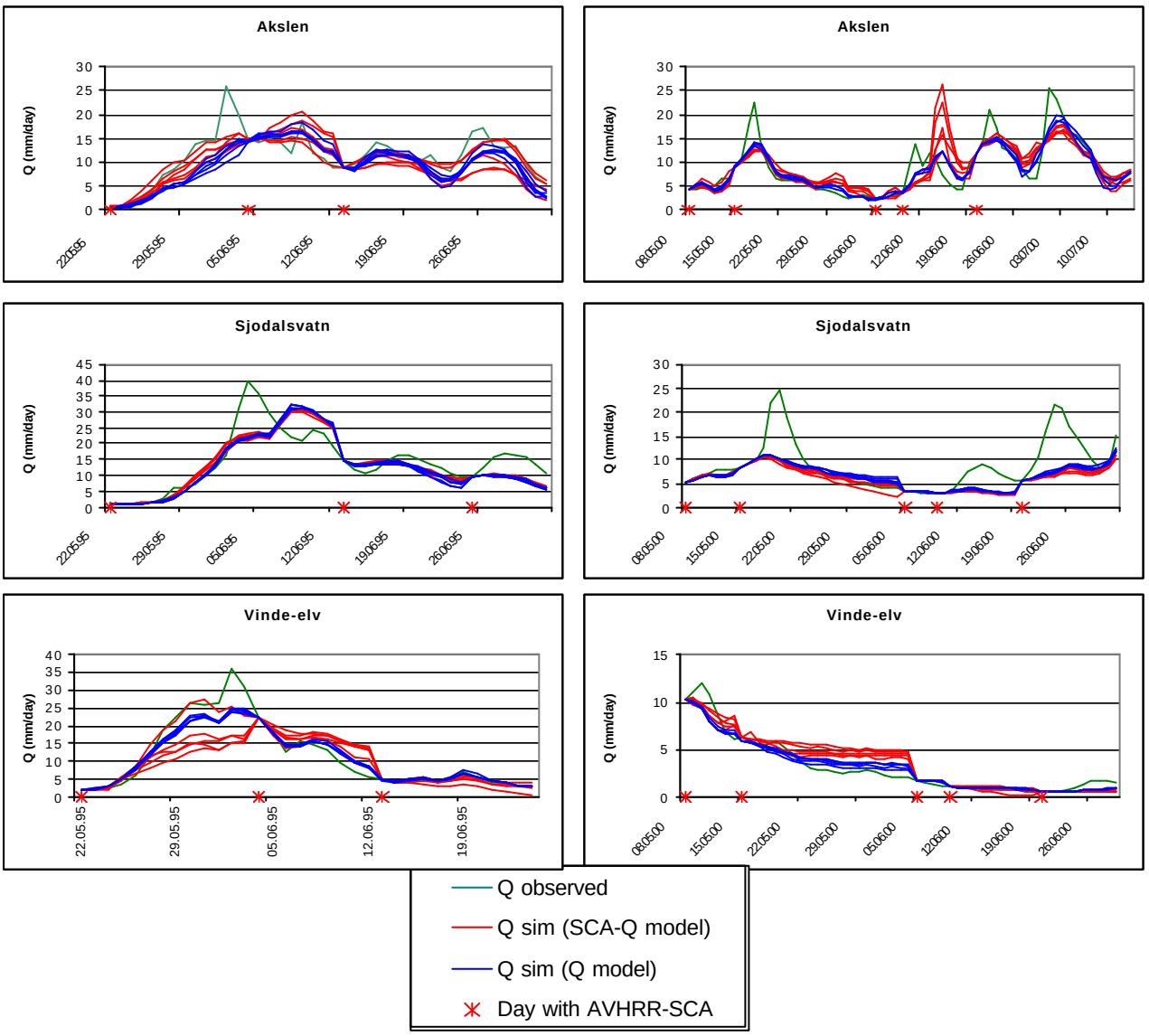

Figure 5: Simulated and observed runoff compared for two of the test years 1995 and 2000.

4.3 Implications to flood forecasting

The calibrations against runoff alone have shown that simulated SCA from the Q models, and AVHRR-derived SCA, differ a lot, even if the runoff is fairly well simulated. In most situations the simulated SCA is much higher than the AVHRR-derived SCA. An updating of the states with AVHRR-data in these models would lead to reduced SCA and reduced simulated runoff in the melting period. Since most of the flooding situations seem to be underestimated in the simulations, updating of the SCA in a Q model would not be recommendable in an operational situation. However, the calibrations have shown that it is possible to calibrate HBV models that simulate SCA more in accordance with the AVHRR-derived SCA, without major reductions in the quality of the runoff simulations. There are still uncertainties

connected to the precision of the AVHRR-derived SCA. For catchments like Vinde-elv, snowmelt and the corresponding reduction in snow reflectance, usually starts earlier than on the glaciers. This leads to an underestimation of the SCA. Forested and shadowed areas will also contribute to such an underestimation. These are factors that should be kept in mind when AVHRR-data are used operationally. Hence the AVHRR-derived SCA is less reliable for Vinde-Elv than for the other two, which probably explains the poor calibration results of the SCA-Q models for this catchment.
When several models, calibrated against runoff and SCA, are run operationally, the models that simulate both runoff and SCA reasonable will be trusted in the forecast period. Nevertheless, in the examined simulations (figure 5) neither the SCA-Q models nor the Q models perform noticeably better than the other models during the first 2-3 days after an updating. For a longer forecast period the Q models tend to be slightly better. However, at special occasions as in 1995, some of the SCA-Q models simulate the start of the flood better than the Q models both for Vinde-elv and Akslen. This indicates that SCA-Q models can be used in addition to the traditional Q models. The precision of the utilised method of deriving SCA from AVHRR images is probably too low for most catchments. Updating of the SCA in the simulations will therefore only be of interest when there are obvious errors in the simulations. Such errors could be simulations of snow free catchments when snow covered areas are derived from AVHRR data. Situations like that are not included in the data sets in this work. Another implication of the simulation results is that the model calibration should be weighted more against the flooding situations. At least for Sjodalvatn, other model calibrations should be used in flooding situations than in a normal forecast situation.

5 CONCLUSIONS

When HBV models are calibrated traditionally, against runoff alone, the simulated SCA tends to be clearly overestimated compared to the AVHRR-derived SCA. Calibrations against AVHRR-derived SCA, in addition to runoff, show that models can be calibrated to simulate SCA more consistently with these data, without major reduction in the precision of the runoff simulations. Models calibrated against SCA and runoff do not prove to simulate runoff better, nor worse, than the traditionally calibrated models during the first days next to an updating of SCA and runoff. As the precision of the utilised method of deriving SCA from AVHRR images probably is too low for most catchments, updating of the SCA in the simulations will only be of interest when there are obvious errors in the simulations.

6 FURTHER WORK

Future work will integrate satellite-derived snow parameters in ten operational HBV models representing different regions and catchment scales in Norway. The model will be adapted to use earth observation data for updating the snow variables snow covered area, snow water equivalent, snow liquid water, surface reflectance and temperature, and model performance and uncertainty will be assessed. A new description of the snow distribution in the HBV model will be developed and tested.

ACKNOWLEDGEMETS

This research takes part of the technical and methodological development of the national flood forecasting service at NVE. NVE is partner in one application development project, DemoSnø, and two research projects on snow remote sensing and modelling, in which scientific advances are translated into improved public services, SnowMan and EnviSnow. Financial support for this work was provided under project contracts SnowMan (co-funded by Norwegian Research Council), DemoSnø (co-funded by Norwegian Space Centre), EnviSnow (co-funded by under the EC 5th framework programme), and research and development funding provided by the Norwegian Water Resources and Energy Directorate.

REFERENCES

1. Bergström, S. 1992. The HBV model-its structure and applications, SMHI Hydrology, RH no.4, Norrköping, 35 pp.

2. Guneriussen (ed.), Per Ludvig Bjerke, Martti Hallikainen, Daniel Hiltbrunner, Harald Johnsen,Ville Jääskeläinen, Sjur A. Kolberg, JarkkoKoskinen, Christian Matzler, Jouni Pulliainen, Knut Sand, Rune Solberg, Andy Standley and Andreas Wiesmann. 2000. Research and development of earth observation methods for snow hydrology - SnowTools Final Report, NORUT Report, ISBN 82-7747-107-6.
3. Rott H. et al. 2000. HYDALP, Hydrology of Alpine and High Latitude Basins, Final Report.Institut für Meteorologie und Geophysik, Universität Innsbruck, Mitteilungen Nr. 4, 2000.
4. Rango, A. and Shalaby, A.I. 1999. World Meteorological Organization Operational hydrology report No. 43, Current operational applications of remote sensing in hydrology, WMO-No. 884, 73 pp.
5. Sælthun, N.R. 1996. The "Nordic" HBV model. Description and documentation of the model version developed for the project Climate Change and Energy Production. NVE Publication no 7, 1996. 26 pp.
6. Schjødt-Osmo, O. and Engeset R.V. 1997. Remote sensing and snow monitoring: Application to flood forecasting. In Refsgaard JC, Karalis EA (Eds), Operational water management, Proc. EWRA: Copenhagen-97. A. A. Balkema, Rotterdam, pp. 83 – 87.
7. Brebber, L., Doherty, J. and Whyte, P. 1994. PEST – Model Independent Parameter Estimation. Watermark Computing, Corinda – Australia.
8. Seibert, J. 1997. Estimation of Parameter Uncertainty in the HBV model. Nordic Hydrology, 28(4/5), pp. 247 – 262.
9. Kolberg, S., Rinde, T. og Tøfte, L.S. 1999. Automatisk kalibrering av hydrologiske modeller. (Automatic calibration of hydrological models, in norwegian). SINTEF rapport STF22 A99402, 42 s.
10. Engeset R., Sorteberg, H.K. and Udnæs, H.C. 2000. NOSIT Utvikling av NVE's operasjonelle snøinformasjonstjeneste. (NOSIT Developing the operational snow information at NVE, in norwegian). NVE Dokument nr 1, 2000. 46 pp.
11. Udnæs, H.-C., Gotschalk, L., and Guneriussen, T. 2001. EO data in hydrological models. NVE Report no 1, 2001. 16 pp.

Annex 2

HBV model description.

HBV model description

This Annex contains a brief description of the model based on the document "Nordic HBV model Karmen, release 3.14, 95/02/26" by Nils Roar Sælthun. For more background information the reader is referred to S. Bergström: "The HBV model - its structure and applications", SMHI Reports Hydrology No 4, Swedish Meteorological and Hydrological Institute 1992. Details on the evapotranspiration part are found in G.Lindström, M.Gardelin & M.Persson: "Conceptual modelling of evapotranspiration for simulations of climate change effects", SMHI Reports Hydrology No 10, 1994.

General structure

The main structure of the HBV model (Figure 1) is a sequence of submodels:

- snow submodel
- soil moisture zone
- dynamic part
- routing

The model is further structured in altitude intervals. This subdivision can be applied only to the snow submodel, or to the whole model. In the latter case, the height intervals can further be subdivided in one or two vegetation zones and lakes. Even when the model distributed on altitude intervals, the parameters are generally the same for all submodels. Interception, snow melt parameters and soil moisture capacity can however be varied according to vegetation type. The model can operate with up to 15 vegetation types, but usually not more than two or three would be activated.

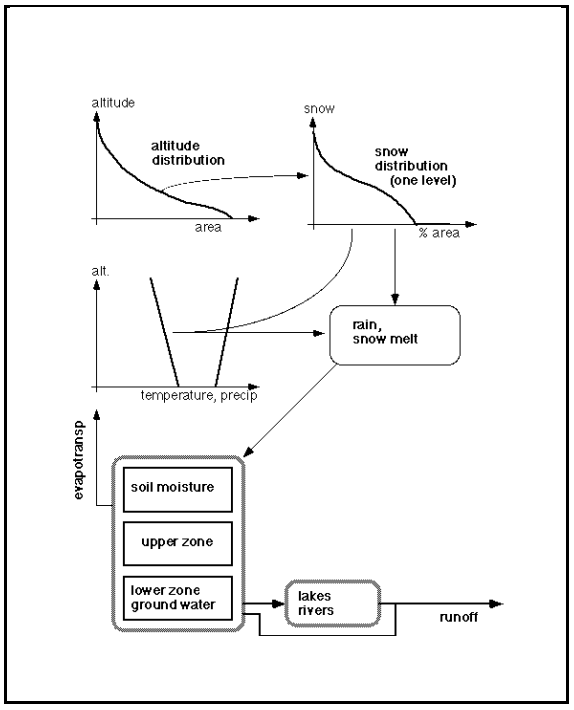

Figure 1 The HBV model.

The distribution of the model in zones is controlled by index #27. Some of the model features described below do only apply to the distributed model.

Precipitation and temperature adjustments

Precipitation adjustment

All precipitation is adjusted by a fixed correction, PKORR, parameter # 45. This adjustment is partly due to gauge catch losses, partly due to nonrepresentative stations (disregarding altitude variations). When the temperature at the observation station indicates snow fall (at the station or at the weighted average altitude of the stations), the precipitation is in addition adjusted with the snow fall correction factor SKORR, #46, to corrected for the larger catch losses for snow.

Temperature and precipitation altitude gradients

The precipitation altitude gradient is assumed to be linear, i.e., a fixed proportional change of the observed precipitation per 100 m altitude. The gradient is PGRAD, #65. An example: PGRAD = 0.03 indicates 3% precipitation increase, of observed precipitation, per 100 m. The gradient can be changed at a specified level, GRADALT, #47, where it changes to PGRAD1, #48. PGRAD1 specifies the change as a proportion of the precipitation at GRADALT. If GRADALT is zero, the change of gradient is not activated.

The temperature gradient is given as a lapse rate, deg C change per 100 m. The lapse rate on days without precipitation is specified by parameter TTGRAD, #63, and on days with precipitation by parameter TVGRAD, #64. Default values are -0.6 deg/100 m.

A seasonal profile of the temperature gradient can be specified by parameters 101 to 112, one per month from January to December. This profile is normalized against TTGRAD and TVGRAD, so that the annual mean value (average of the monthly values) equals these.

Snow submodel

Snow accumulation

Snow accumulation in an altitude level starts when precipitation falls at temperature lower than TX, #40. Up to an accumulated storage of SPDIST, #113, the accumulation is even. When the storage reaches this level, additional snow fall is distributed according to the specified snow distribution.

Snow distribution

Snow distribution is given as a lognormal distribution, calculated for the quantile intervals 0.0-0.01, 0.01-0.05, 0.05-0.15, 0.15-0.35, 0.35-0.65, 0.65-0.85, 0.85-0.95, 0.95-0.99 and 0.99-1.0. In one altitude zone, this will give the following possibilities for snow cover percentage: 0, 1, 5, 15, 35, 65, 85, 95, 99, 100 %. The actual form of the snow distribution is specified by its

coefficient of variation, parameter CVMAX in the VEGTYPE file. Some examples of distributions for typical values of CVMAX are given in Figure 2.

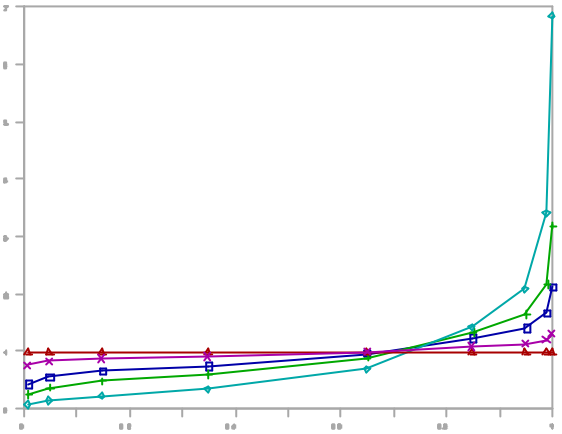

Figure 2. Snow distribution.

Snow melt and refreeze

Basically the HBV model uses a temperature index (degree-day) method for snow melt calculation. The temperature index melt equation is

$M = CX \cdot (T - TS)$ for $T > TS$

$M = 0$ " $T < TS$

where M is the melt (in mm), T is the altitude level temperature during the time step, TS the threshold temperature, parameter #41, and CX the temperature index, #40.

Meltwater is retained in the snow until the amount of liquid water reaches a fraction LV (parameter #44). Over this threshold meltwater leaves the snow pack. All nine subdivisions of the snow distribution in an altitude zone are treated individually.

When the temperature is below the melt threshold temperature, liquid water in the snow pack will refreeze, but at a lower efficiency than the melt. The refreeze equation is

$F = CFR \cdot CX \cdot (TS - T)$ for $T < TS$

$F = 0$ " $T > TS$

CFR, #43, is a dimensionless constant less than 1.

Albedo simulation, varying temperature index

A simulation option allows varying temperature index, depending on whether is rains or not, and on albedo. This option is activated by setting index #29 to 1.

Albedo simulation. The albedo simulation is based on snow aging. The limiting values for the albedo are depending on the snow liquid water content - the maximum value is varying linearily from 0.5 for fully saturated snow to 0.8 for dry snow, and the minimum value from 0.2 for fully saturated to 0.6 for dry snow. More than 5 mm of snow fall will lift the albedo to the maximum value. Otherwise the albedo will fall towards the limiting lower value by a temperature dependent exponetial decay. The decay factor is specified by the parameter CALB, #49. The new albedo is calculated by the equation

$A_{t+1} = A_{min} + (A_t - A_{min}) \cdot (1 - CALB \cdot T)$

for days with temperature higher than 0.

For days with temperature between -10 ºC and 0, the albedo is also reduced, but by a factor only five per cent of the decay for temperatures higher than zero.

Temperature index. For simulations with varying temperature index, the temperature index is split in three parts by the three parameters CRAD, CCONV and CCOND, #50, #51 and #52.

"Radiation" part: The "radiation" part is depending on albedo, potenital short wave radiation at the earth surface, and precipitation. The short wave radiation is calculated by astronomical formulas, and is depending on the latitude, LAT, #100, and the day number. The actual radiation melt temperature index is calculated by the formula:

$CX_{rad} = CRAD \cdot CX \cdot RVEKT \cdot e^{-0.1 \cdot P}(1-A)/0.5$

RVEKT is the normalized potential infalling radiation, set to 1 at May 15 at 60o N. RVEKT will vary from 0.05 at Jan 1 to 1.15 at midsummer. P is the precipitation. The component varies linearly with albedo and decreases exponentially with precipitation. At 10 mm it is reduced to 37% of the value at days without precipitation.

"Convection" part: The "convection" temperature index is always active, and equals

$CX_{conv} = CCONV \cdot CX$

"Condensation" part: The "condensation" temperature index is only active during precipitation days (more than 1 mm of rain), and equals

$CX_{cond} = CCOND \cdot CX$

Glacier melt

On glaciers snow accumulates and melts at the same rate as on the non-glacierized areas in the same altitude level. For exposed glacier ice, the melt is increased by a factor CBRE, #66. If albedo-dependent snow melt is used, the albedo of the glacier ice is also set to the lowest value, 0.2.

Glacier snow storage zeroing

To avoid excessive snow storage build up in high areas, above the glaciation limit (the model has no other mechanism for converting "old" snow into glacier ice), any snow storage above the level SPDIST is set to SPDIST at the end of the snow melt season. The liquid water content is reduced accordingly. The day for snow storage reduction is given by the parameter NDAG, #39.

Evapotranspiration, interception

Potential evapotranspiration

Potential evapotranspiration can either be given as parameters to the model, or calculated by a temperature index method. In the first case, average potential evapotranspiration in mm/day is given for each month by parameters EP(1) to EP(12) - #67 to #78 (January to December). These are used as fixed

values, and there is no differentiation between altitude levels or vegetation zones.

By the temperature index method, the potential evapotranspiration is calculated for each time step using a simple temperature index method:

$PE = CE \cdot T$ for $T > 0$

$PE = 0$ for $T < 0$

CE is specified by parameter #98. In addition, the potential evapotranspiration can be given a seasonal profile - the parameters #67 to #78 will in this mode act as monthly correction factors for CE. This seasonal profile can further be modified by the vegetation parameter EPVAR. The final temperature index formula is

$PE = CE \cdot T \cdot (1+(EP(mnd)-1) \cdot EPVAR)$

The mode for evapotranspiration calculations is controlled by index #25.

Snow evaporation

Generally, only snow free areas are assumed to evaporate. An exception is intercepted snow - see below.

Lake evaporation

Lakes are assumed to evaporate at potential rate. Parameter #60, CEVPL, is an adjustment on "land" evaporation as described above, to be applied on lakes. If preset potential evaporation is used, lakes are assumed to be icecovered to the same extent as the adjacent ground is snow covered. If temperature index metods are used, then the lake evapotranspiration is based on a simulated lake temperature. The lake temperature is calculated by a simple autoregressive model:

$$TLAKE_t = TLAKE_{t-1}(1 - 1/TLDAY) + T_t/TLDAY$$

where TLAKE is lake surface temperature and T is air tempertature. TLDAY is a parameter describing the temperature "memory" in days. If TLDAY (#62) is 0 or 1 then lake temperature is equal to air temperature. Lake evaporation is calculated by the equation

$E_{lake} = CEVPL \cdot CE \cdot TLAKE$ for $TLAKE > 0$

$E_{lake} = 0$ for $TLAKE < 0$

This is a lake evapotranspiration method for shallow lakes developed at SMHI.

Interception

Interception storage is specified by the vegetation parameter ICMAX - given in mm. The interception storage will loose water at potential evapotranspiration rate, regardless of whether the intercepted precipitation is rain or snow. As long as water is present in interception storage, the actual evapotranspiration from the soil moisture zone is reduced by $EP \cdot ERED$, where ERED is a dimensionless constant less than 1 specified by parameter #61.

Soil moisture zone

A central part of the HBV model is the soil moisture zone. Metwater from snow, rain on snow free areas and glacier ice melt is input to this zone. In addition

water can be drawn up from the ground water zone to the soil moisture zone. Actual evapotranspiration is calculated on the basis of the water content im this zone, and the percolation to the dynamical parts of the model is a function of the water content. Water percolated "through" the zone is not delayed, and water is only removed from the zone by evapotranspiration.

Actual evapotranspiration

Actual evapotranspiration is calculated by the equation

$AE = PE \cdot SM/(FC \cdot LPDEL)$ for $SM < FC \cdot LPDEL$

$AE = PE$ for $SM > FC\ LPDEL$

where SM is actual soil moisture content, FC (#79) is the maximum water content of the zone (in mm), and LPDEL (#80) a dimensionless parameter (< 1), indicating the level at which the evapotranspiration is potential. FC as given in the main parameter file can be adjusted by the FCVEG parameter in the vegetation description file (VEGTYPE.DAT) - the actual vegetation zone maximum soil moisture content will be FC FCVEG. The LPDEL parameter in the main parameter file can be overridden by the LPDEL parameter in the VEGTYPE file.

Maximum infiltration

A maximum input rate to the upper zone can be specified by the parameter INFMAX, #82, in mm/d. The part of the input exceeding this will go directly to the upper zone.

Percolation

A fraction of the input water is percolated on to the dynamic parts of the model. The fraction percolated is given by the equation

$CUZ = INSOIL \cdot (SM/FC)^{BETA}$ for $SM < FC$

$CUZ = INSOIL$ for $SM = FC$

a nonlinear relationship controlled by the BETA exponent, parameter #81.

Draw up

Water can be drawn from the ground water zone to the soil moisture zone. The amount drawn up is given by the equation

$UP = 2.0\ DRAW \cdot (LZ/LZMAX) \cdot (FC-SM)/FC$

where DRAW is the parameter controlling the draw up. It is given in mm/d, and is the draw up when the soil moisture zone is at $0.5 \cdot FC$, and the ground water content (LZ) is at maximum (LZMAX).

Upper zone

The upper zone is, together with the routing module, the main dynamical part of the model. It is essentially a piecewise linear reservoir, but with a constant deep percolation to the ground water zone - as long as there is water in the upper zone.

Deep percolation

The deep percolation to the lower zone is controlled by one parameter, PERC - #88 - given in mm/d.

Dynamic response

The zone has a two level dynamic response, controlled by three parameters, KUZ1 (#87), UZ1 (#86) and KUZ2 (#85). KUZ and KUZ1 are response coefficients in unit d^{-1}, and UZ1 is a threshold level between the two response regimes, given in mm. The response is essentially

$QUZ = KUZ1 \cdot UZ$ for $UZ < UZ1$

$QUZ = KUZ2 \cdot (UZ-UZ1) + KUZ1 \cdot UZ1$ for $UZ > UZ1$

This is the momentarily response - in the actual calculation these equations are integrated over the time step. Approximations of the following type is used:

$$QUZ = (UZ+0.5(CUZ-PERC)) \cdot 2.0 \cdot KUZ/(2.0+KUZ)$$

where UZ is the content of the upper zone at the start of the time step, and CUZ-PERC is the inflow to the zone.

Lower zone

The lower zone is a linear reservoir, describing ground water response. The runoff from the zone is given by

$$QLZ = KLZ \cdot LZ$$

where LZ is the lower zone content (mm), and KLZ (#89) the response coefficient. AS the inflow to the zone is limited to PERC (mm/d), the outflow will balance inflow at a content of

$$LZMAX = PERC/KLZ$$

A linear reservoir will never empty by runoff, but the draw up mechanism (3.5.4) can empty it, permitting periods with zero runoff from the model.

Lakes

Lake percentage is specified in each altitude interval. Precipitation on lakes and lake evaporation are calculated for each altitude interval, but the dynamic response of the lake area is calculated aggregated for the catchment. All preciptiation on lakes, regardless whether it is rain or snowfall, is a direct contribution to the lake water balance. If there are reservoirs in the catchment, specified by MAGDEL, #4, the precipitation minus evaporation on this part of the lake area is added directly to runoff. The rest of the lake net precipitation is attenuated by the lake dynamics.

Lake dynamics

The lake dynamics are described as a single lake, through which the net lake precipitation and a part of the catchment runoff is routed. The parameters for the lake routing is:

KLAKE	#56	the rating curve coefficient of the lake
DELH	#57	the zero point of the rating curve
NLAKE	#58	the rating curve exponent

DELF #59 the part of the catchment (runoff) that drains through the lake

Routing

Runoff from the dynamic part of the model (upper zone, lower zone, lake dynamics) can be attenuated/delayed throug the routing module. Three methods of routing is available, specified by index #22. The three methods are:

0: no routing
1: lake routing
2: smoothing with fixed weights
3: smoothing with discharge dependent weights (triangular unit hydrograph)

The routing parameters are the five parameters ROUT(1) to ROUT(5), #90 to #94. The actual interpretation depends on the routing method chosen.

Lake routing

This routing corresponds to the lake dynamics described above. Lake dynamics and lake routing can be combined to simulate two lakes in series.

ROUT(1) lake area (km^2)
ROUT(2) lake rating curve coefficient
ROUT(3) rating curve zero
ROUT(4) rating curve exponent
ROUT(5) part of catchment (runoff) draining through lake

Fixed weights routing

This is a moving average type routing with up to six weights:

$$Q_i = W1 \cdot QI_i + W2 \cdot QI_{i-1} + ... + W6 \cdot QI_{i-5}$$

where QI is the input to the routing. Parameter interpretation:

ROUT(1) W1
ROUT(2) W2
ROUT(3) W3
ROUT(4) W4
ROUT(5) W5

W6 is calculated as 1 - W1-W2-W3-W4-W5.

Discharge dependent weights

This is routing by a triangular unit hydrograph, with discharge dependent base (the original HBV routing). Parameter interpretation:

ROUT(1) Q1
ROUT(2) T1
ROUT(3) Q2
ROUT(4) T2

T1 is time base for discharge level Q1, while T2 is time base for discharge Q2. The actual time base is interpolated (or extrapolated) from (Q1,T1), (Q2,T2). The maximum time base is five time steps (days). If the extrapoation gives a higher value, it is set to five days.

Error functions

In single simulations, error topography and optimization run mode, error functions are presented to support interpretation of the results. It should be emphasized that the best judgment of the parameter fit very often is obtained by visual inspection of a graphical display of the simulations. The simulated water balance is also a very important guidance in model calibration, as are duration curves and frequency analysis of observed and simulated data. Duration curve and frequency analysis is not presented by the model software, but can easily be produced by for instance spreadsheet programming, utilizing the data output produced by the model.

The error functions produced by the model is:
F2 is simply the sum of squares of the errors (in mm/d). It is always non-negative, and a perfect fit gives F2=0. The smaller the better.

R2 varies from minus infinity to 1. 1 indicates perfect fit. An R2 value of 0 is a model as good (or bad) as setting the simulated value constant to the mean runoff. An R2 value of 0.8 usually indicates what would be regarded a fairly good fit.

F2 and R2 are very sensitive to flood values - due to the second power involved, and timing errors in floods will affect these criteria strongly.

What is indicated in the output file as *rel.diff***2 is: The *R2-log* error function corresponds to the R2 error function, but calculated on the logaritms of the observed and simulated runoff, to give more weight to the low flow data (this corresponds loosely to making the analysis on relative errors instead of absoulute errors). The runoff data are given an increment of 0.001 mm day to avoid problems in period with zero runoff.

What is listed in the output as *Difference* is simply the difference between simulated and observed runoff over the whole period - in mm. It cnt be used for optimization - a good fit should give a low difference, but a low accumulated difference does not ensure a good fit

Denne serien utgis av Norges vassdrags- og energidirektorat (NVE)

Utgitt i Oppdragsrapportserie A i 2002

Nr.1 Roger Sværd: Flom – og vannlinjeberegning for Futelva ved Bodø (165.2Z)
Kartlegging av flomfare ved indre Bertnes bru (32 s.)

Nr. 2 Panagiotis Dimakis: Grunnvannsundersøkelser i Røvassdalen og Glomåga
Oppsummering av grunnvannsundersøkelser (66 s.)

Nr. 3 Roger Sværd: Normalvannstand i Storvann nord, Harstad kommune (30 s.)

Nr. 4 Hervé Colleuille: Skurdevikåi tilsigsfelt (015.NDZ) Grunnvannsundersøkelser
Årsrapport 2001 (18 s.)

Nr. 5 Hervé Colleuille: Filefjell - Kyrkjestølane (073.Z). Grunnvannsundersøkelser
Årsrapport 2001 (15 s.)

Nr. 6 Rune V. Engeset and Hans-Christian Udnæs: Satellite-observed Snow Covered Area
in the HBV-model. Final report The DemoSnow project (32 s.)